



## Connecting molecular biomarkers, mineralogical composition, and microbial diversity from Mars analog lava tubes

Vera Palma<sup>a,1</sup>, José L. González-Pimentel<sup>a,1</sup>, Nicasio T. Jimenez-Morillo<sup>b</sup>, Francesco Sauro<sup>c</sup>, Sara Gutiérrez-Patricio<sup>b</sup>, José M. De la Rosa<sup>b</sup>, Ilaria Tomasi<sup>d</sup>, Matteo Massironi<sup>d</sup>, Bogdan P. Onac<sup>e,f</sup>, Igor Tiago<sup>g</sup>, José A. González-Pérez<sup>b</sup>, Leonila Laiz<sup>b</sup>, Ana T. Caldeira<sup>a</sup>, Beatriz Cubero<sup>b</sup>, Ana Z. Miller<sup>b,a,\*</sup>

<sup>a</sup> HERCULES Laboratory, University of Évora, Évora, Portugal

<sup>b</sup> Instituto de Recursos Naturales y Agrobiología de Sevilla (IRNAS-CSIC), Sevilla, Spain

<sup>c</sup> Department of Earth Sciences and Environmental Geology, University of Bologna, Italy

<sup>d</sup> Geosciences Department, University of Padova, Padova, Italy

<sup>e</sup> Karst Research Group, School of Geosciences, University of South Florida, Tampa, FL, USA

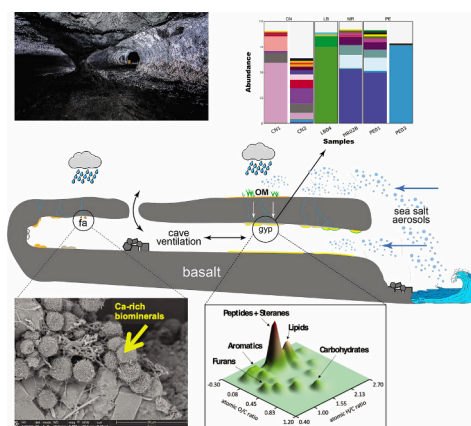
<sup>f</sup> Emil G. Racoviță Institute, Babeș-Bolyai University, Cluj-Napoca, Romania

<sup>g</sup> CFE-Center for Functional Ecology, Department of Life Sciences, University of Coimbra, Coimbra, Portugal

### HIGHLIGHTS

- Lanzarote is a remarkable Martian volcanology analog, with lava tubes potentially containing biosignatures.
- Unique bacteria in oceanic-influenced conditions contribute to cave mineral formations and organic records.
- Role of the bacterium *Crossiella* in precipitating biosignificant Ca-rich fluorapatite
- PCA analysis links organic compounds, microbial taxa, and minerals.

### GRAPHICAL ABSTRACT



### ARTICLE INFO

Editor: Daniel Alessi

#### Keywords:

Volcanic caves  
Speleothems

### ABSTRACT

Lanzarote (Canary Islands, Spain) is one of the best terrestrial analogs to Martian volcanology. Particularly, Lanzarote lava tubes may offer access to recognizably preserved chemical and morphological biosignatures valuable for astrobiology. By combining microbiological, mineralogical, and organic geochemistry tools, an in-depth characterization of speleothems and associated microbial communities in lava tubes of Lanzarote is

\* Corresponding author at: IRNAS-CSIC, Seville, Spain.

E-mail address: [anamiller@irnas.csic.es](mailto:anamiller@irnas.csic.es) (A.Z. Miller).

<sup>1</sup> These authors have contributed equally to this work.

Geomicrobiology  
 Biosignatures  
 Biomarkers  
 Organic matter  
 Subsurface microbial communities  
 Biomineralization

provided. The aim is to untangle the underlying factors influencing microbial colonization in Earth's subsurface to gain insight into the possibility of similar subsurface microbial habitats on Mars and to identify biosignatures preserved in lava tubes unequivocally.

The microbial communities with relevant representativeness comprise chemoorganotrophic, halophiles, and/or halotolerant bacteria that have evolved as a result of the surrounding oceanic environmental conditions. Many of these bacteria have a fundamental role in reshaping cave deposits due to their carbonatogenic ability, leaving behind an organic record that can provide evidence of past or present life. Based on functional profiling, we infer that *Crossiella* is involved in fluorapatite precipitation via urea hydrolysis and propose its Ca-rich precipitates as compelling biosignatures valuable for astrobiology.

In this sense, analytical pyrolysis, stable isotope analysis, and chemometrics were conducted to characterize the complex organic fraction preserved in the speleothems and find relationships among organic families, microbial taxa, and precipitated minerals.

We relate organic compounds with subsurface microbial taxa, showing that organic families drive the microbiota of Lanzarote lava tubes. Our data indicate that bacterial communities are important contributors to biomarker records in volcanic-hosted speleothems. Within them, the lipid fraction primarily consists of low molecular weight *n*-alkanes,  $\alpha$ -alkenes, and branched-alkenes, providing further evidence that microorganisms serve as the origin of organic matter in these formations. The ongoing research in Lanzarote's lava tubes will help develop protocols, routines, and predictive models that could provide guidance on choosing locations and methodologies for searching potential biosignatures on Mars.

## 1. Introduction

Terrestrial volcanic eruptions produce large amounts of magma-derived products such as hot lava, volcanic ash, and gases. Effusive eruptions often form lava tubes, which have even been reported on the Moon and Mars (Greeley, 1971; Haruyama et al., 2009; L  veill   and Datta, 2010; Sauro et al., 2020). Despite having low nitrogen and organic carbon levels, lava tubes on Earth are rapidly colonized by microorganisms (Biderre-Petit et al., 2020; Kelly et al., 2014), whose growth is fueled by surface-derived organic matter transported along rock discontinuities via dripping water or by CO<sub>2</sub> fixed in situ by chemolithoautotrophic organisms (Selensky et al., 2021). Jelly-like speleothems in a lava tube from La Palma Island (Spain) have been found to be composed of amorphous aluminum silicate matrix and pyrogenic organic matter from the overlying burnt forest (Miller et al., 2020a). In lava tubes from the Galapagos (Ecuador), Miller et al. (2020b) revealed a highly diverse bacterial composition, dominated by *Actinomycetota* and *Pseudomonadota*, mainly influenced by anthropogenic activities and changes in land use, leading to significant alterations in speleothem chemistry (Miller et al., 2022). In contrast, Lavoie et al. (2017) demonstrated that cave microbial diversity in tubes from Lava Beds National Monument (USA) differed significantly from that found in the overlying surface soils. Although previous studies showed the influence of land use and geochemical conditions on subsurface microbial communities, there are still several open questions on the differential colonization of lava tubes, depending, among other factors, on surface nutrients and environmental settings, depth of the conduits, age of formation and exposure to water percolation. Studying these Mars-like geological sites on Earth is fundamental for understanding Martian paleoenvironments, search for biosignatures and for establishing strategies for its exploration and habitability conditions (L  veill   and Datta, 2010; Mart  nez-Fr  as et al., 2006; Mart  nez-Fr  as, 2014). Biosignatures are evidences of the presence of life and their metabolic processes and can include morphological features, such as microfossils, biominerals and imprints of microbial cells on mineral substrates (Westall et al., 2006; Westall et al., 2015), or chemical and isotopic biosignatures, as organic compounds (e.g., lipids, amino acids produced by biological activity), changes in trace element distributions (Leslie et al., 2013), and the isotopic composition of breakdown products of organic matter (Westall and Cavalazzi, 2011). Multiple analytical techniques are currently being utilized to search for organic compounds on Mars and their analogs (Huidobro et al., 2022). These methods include Fourier-transform infrared spectroscopy (FT-IR), Raman spectroscopy, and fluorescence spectroscopy, which are already in use on the Perseverance Rover (Ansari, 2023; Baqu   et al., 2022). Since 1975, with the Viking

mission, analytical pyrolysis has been the main methodology for studying organic compounds in Martian (sub-) surface materials. In particular, the Mars Organic Molecule Analyzer (MOMA) on the Exo-Mars rover relies on Pyrolysis-Gas Chromatography/Mass Spectrometry (Py-GC/MS) to detect organic molecules on Mars, intending to identify potential traces of present or past life (Reinhardt et al., 2020). This technique enables the analysis of organic compounds preserved in the mineral fraction without the need for sample pre-treatment. This presents a significant analytical advantage due to the impossibility of conducting molecular extraction procedures on Mars. However, pyrolysis may thermally destroy and transform organic matter, depending on the temperature and nature of the molecules, thus altering their original molecular signatures (Reinhardt et al., 2020). Therefore, studying terrestrial analogs is crucial for fully understanding: i) how biosignatures are formed, preserved, degraded, and potentially detected in Martian materials, and ii) the analytical alteration mechanisms of organic molecules produced by analytical pyrolysis.

Lanzarote, in the Canary Islands, Spain, offers one of the best terrestrial analogs to Martian volcanoes, due to its basaltic lava flow composition, surface aridity, and salt brines (Supplementary Information; Meyzen et al., 2015; Mart  nez-Fr  as et al., 2017; Mateo-Mederos et al., 2019; Sauro et al., 2023). The lava fields of Lanzarote, in particular, hold an astounding array of cavities with several similarities to lava tube collapses and other volcanic cave structures identified on the Moon and Mars (Carr and Head, 2010; Blair et al., 2017; Sauro et al., 2019). These exceptional planetary analog sites offer unique opportunities to planetary caves research, to test new approaches for future planetary missions, and to better understand the geological and potential microbial processes on Mars subsurface (Miller et al., 2018; Sauro et al., 2023). All astrobiological studies that have been carried out in Lanzarote are mainly focused on comparative planetology studies about primary and secondary minerals, volcanic and sedimentary outcrops, geomorphology of volcanic edifices, and genesis of lava tubes (Sauro et al., 2020, 2023).

This study provides a comprehensive analysis of microbial communities associated with secondary mineral deposits in Lanzarote lava tubes, to understand relationships between mineralogy, molecular composition, and subsurface microbial life, exploring the minerals-organics-microbes link in both subaerial and underground geology and mineralogy. The aim is to untangle factors that drive subsurface microbial colonization on Earth to better understand the potential for analog extraterrestrial subsurface microbial habitats on Mars and beyond. Additionally, as Lanzarote lava tubes may preserve recognizable chemical and morphological biosignatures valuable for astrobiology, this research contributes to identifying potential biosignatures

within Mars analog lava tubes.

## 2. Materials and methods

### 2.1. Sampling sites and methods

In May 2021, a sampling campaign was conducted in four lava tubes from Lanzarote. A detailed description of the caves, including their geology, formation, location and environmental conditions is presented in the Supplementary Information. Table 1 and Fig. S1 provide a summary of their location, relevant information and samples analyzed at each lava tube.

After a very detailed examination of the different sets of underground environments, six microbiologically relevant niches were identified for this study. From each sampling site, five replicate samples of secondary mineral deposits or colored microbial mats were collected for DNA-based analysis, culture procedures, microscopy, mineralogy, and biogeochemistry investigations (Table 1). Samples were aseptically collected using sterile scalpels and stored in sterile 50 mL tubes or Whirl-Pak® sample bags. All samples were kept at 4 °C until transportation to the lab. Samples for DNA-based analyses were stored at −80 °C until laboratory procedures. All samples were collected from the dark zone of the lava tubes, apart from sampling sites MR02, which is situated close to a roof collapse, and PE01, which was collected about 30 m from the lower exit of the tube, therefore receiving some faint indirect light during the day. Both sampling sites exhibited green patinas coating white secondary mineral deposits (Table 1).

### 2.2. Morphological and mineralogical characterization

To accurately detect microbial cells, characterize their morphology, and provide a mineralogical context for the collected speleothem samples, field emission scanning electron microscopy (FESEM), X-ray diffraction (XRD), and Raman analysis were performed.

Field Emission Scanning Electron Microscopy (FESEM) with Energy Dispersive X-ray Spectroscopy (EDS) was conducted to detect microbial

cells and characterize their morphology. Small fragments of each sample were air-dried, mounted on sample stubs, and sputter-coated with a thin palladium film. Subsequently, samples were examined using a FEI Teneo FESEM (FEI Company, Eindhoven, The Netherlands) with the secondary electron detection mode and an acceleration voltage of 5 kV for ultra-high-resolution images.



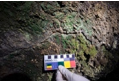



To provide a mineralogical context for the collected speleothem samples, X-ray diffraction (XRD) and Raman analyses were performed. Bulk samples were ground into fine powder and analyzed using a Philips X'Pert Pro MPD diffractometer (Malvern Panalytical Ltd., Malvern, UK) at the Department of Earth Sciences of the University of Padova (Italy) for mineralogical investigations. The instrument utilizes a long-fine-focus cobalt anode tube running at 40 kV–40 mA and a 240 mm goniometer radius operating in the  $\theta/\theta$  geometry. A Bragg-BrentanoHD (BBHD) module with W/Si wafer crystal improves signal-to-noise and peak-to-background ratios while reducing  $K\alpha$ -2 and  $K\beta$  lines. The total scan time is 1 h and 6 min. Measures were conducted between 3° and 85° 2 $\theta$  angle, using a 0.017° step size, counting 100 s per virtual step on a circular, 27 mm diameter, spinning sample (1 revolution per second). Powder samples were prepared using the back-loading procedure to minimize crystallites' preferred orientations. Mineralogical species were identified using PANalytical High Score Plus v.4.9.0 software (Malvern Panalytical Ltd., Malvern, UK).

In addition to XRD, some mineral grains in each sample were identified by means of a preliminary binocular microscope examination at 20–60 X; the most significant of them were analyzed by the Micro-RamanSpectra team (Padova) using a Raman XploraPlus® analysis apparatus with a 532 nm laser by Horiba Ltd. The Raman dataset was compared with spectra in databases and literature using Crystal Sleuth® software, developed during the RRUFF TM Project of the Department of Geosciences at the University of Arizona (Lafuente et al., 2015).

### 2.3. Microbial diversity and function

High-throughput sequencing of 16S rRNA gene amplicons of the six sampling sites was performed to provide a detailed characterization of

**Table 1**  
Studied lava tubes and samples description.

Cave name	Development (m)	Ref. and surveys	Sample ID	Sample description	Photo
Cueva de Los Naturalistas	1647	GIE-UL (Martín and Díaz, 1984), GES-CMB (Montoriol et al., 1991)	CN1	White microbial mats coating the lava substrate	
			CN2	Whitish coralloid-type speleothems	
Montaña Rajada	168	Timanfaya National Park inventory	MR02	Green patinas on white secondary mineral deposits on the cave wall	
Paso Esqueleto	550	Timanfaya National Park inventory	PE01	Green patinas associated with white secondary mineral deposits on the cave wall	
			PE03	White gypsum-like deposits on rock fracture	
Cueva Las Breñas	2184	Vulcanfaya Vertical - Speleo NL 2017	LB04	White microbial-like colonies on the lava substrate	

the bacterial communities and predict their functional abundances.

Genomic DNA was isolated from 250 to 500 mg of sample material using the DNeasy PowerLyzer PowerSoil Kit according to the manufacturer's protocol (Qiagen, Venlo, The Netherlands) and quantified using a Qubit 4.0 fluorometer (Invitrogen, Thermo Fisher Scientific, USA). Blank controls were included for all DNA extractions. The extracted DNA was then used as template for Polymerase Chain Reaction (PCR) amplification targeting the 16S rRNA gene using the primer pair 616F (5'-AGAGTTTGATYMTGGCTCAG-3'; Juretschko et al., 1998) and 1510R (5'-GGCTACCTTGTACGACTT-3'; Echigo et al., 2005) for bacterial community analysis, and the primer pair 109F (5'-ACKGCTCAGTAA-CACGT-3') and 915R (5'-GTGCTCCCCGCCAATTCCT-3') for archaea (Großkopf et al., 1998). The internal transcribed spacer (ITS) region was also amplified using the specific primers ITS1 (5'-TCCGTAGGT-GAACCTGCGG-3') and ITS4 (5'-TCCTCCGCTTATTGATATGC-3') for fungal community analyses (White et al., 1990). PCR reactions were performed in a Biometra thermocycler T-Gradient ThermoBlock (Göttingen, Germany) using the following cycling program: 94 °C for 2 min; 35 cycles of 94 °C for 20S, 55 °C for 20S, 72 °C for 2 min; and the final step of 72 °C for 10 min. The amplified products were assessed by electrophoresis on 1 % (w/v) agarose gels, stained with SYBR Safe DNA Gel Stain (Carlsbad, USA) and visualized under UV light. The primer pairs used for archaeal and fungal community analyses yielded no PCR products. Hence, the extracted DNA was sequenced to characterize the bacterial communities dwelling in the lava tubes using the metabarcoding data analysis. For this purpose, the V3–V4 fragment of the 16S rRNA gene was amplified by PCR using the region-specific primers 341F - 805R (Thijs et al., 2017; Wasimuddin et al., 2020), and sequenced in a MiSeq platform to produce 2 × 300 bp paired-end reads, according to the Illumina MiSeq Reagent Kit v3 library preparation protocol used by Macrogen Sequencing Services (Seoul, Korea).

Raw data were processed with QIIME2 v.2020.2 following its instructions (Bolyen et al., 2019). The Amplicon Sequence Variants (ASVs) table was created following DADA2 instructions (Callahan et al., 2016). Reads 1 and 2 were truncated to 280 and 267 bp, respectively. SILVA database v.132 was used to assign the taxonomic classification with a cutoff of 97 % (Quast et al., 2013). Shannon and Pielou indices were calculated for statistical evaluation of richness and evenness (Pielou, 1966; Shannon, 1948). Unweighted and weighted variants from the UniFrac metric were obtained for qualitative and quantitative measurement of Beta diversity (Lozupone and Knight, 2005; Lozupone et al., 2007). We evaluated the differences between communities by means of permutational multivariate analysis of variance (PERMANOVA) with 999 permutations. The raw reads are available at the NCBI Sequence Read Archive (SRA) database under accession number PRJNA816077.

Functional profiles were explored using PICRUSt2 (Douglas et al., 2020; <https://github.com/picrust2/picrust2>) following the standard pipeline. This software predicts functional abundances using a database of phylogenetically referenced genomes, based only on marker gene sequences, and in our case, the 16S rRNA gene. This bioinformatic tool predicts gene family abundances (such as KEGG orthologs and Enzyme Classification numbers) based on 16S rRNA gene surveys. For the analysis, we employed the biome data table obtained from DADA2. The accuracy of metagenome predictions depends on how closely related the microbes in each sample are to sequenced genome representatives. This accuracy is measured by the Nearest Sequenced Taxon Index (NSTI), where lower values indicate a closer relationship (Langille et al., 2013). Values with a NSTI score below 2 were not considered. Metabolic pathways were calculated with the Kyoto Encyclopedia of Genes and Genomes (KEGG) database (Douglas et al., 2020) at <https://www.genome.jp/kegg/>, focusing on the presence of genes involved in sulfur, methane, and nitrogen metabolism, as well as CO<sub>2</sub> fixation.

#### 2.4. Cultivation and identification of bacterial strains

To grow viable cells of cave samples, approximately 250 mg of

samples were resuspended in a sterile 0.85 % (w/v) NaCl solution and subsequently plated on nutrient agar (NA), trypticase-soy agar Na—Mg (20 g MgSO<sub>4</sub> × 7 H<sub>2</sub>O and 30 g NaCl for 1 L medium), GYM Streptomyces (DSMZ 65 medium) and agar marine medium (DSMZ 514 medium) for halophile isolation. All samples were incubated at 30 °C for 7 weeks.

Amplification of 16S rRNA gene for strain identification was attempted by PCR using the primer pair 616F/1510R, as described previously. The PCR products were purified and sequenced by STAB VIDA Sequencing Services (Caparica, Portugal). The DNA sequences obtained were edited using Bioedit v7.2.5 software (Technelysium, Tewantin, Australia). The phylogenetic identification was determined using the global alignment algorithm on the EzTaxon-e database (Yoon et al., 2017). The generated 16S rRNA sequences were deposited in GenBank (<https://www.ncbi.nlm.nih.gov/genbank/>) under accession numbers OQ804791 - OQ804805 and OQ805860 - OQ805866.

#### 2.5. Stable isotope analysis and analytical pyrolysis (Py-GC/MS)

The characterization of the organic matter preserved in the speleothems was conducted by elemental and stable carbon isotope analysis, and analytical pyrolysis (Py-GC/MS).

Total carbon content (TC) and stable carbon isotope analysis were determined in-ground and homogenized aliquots of siliceous and gypsum-rich speleothems. Determination of TC in the speleothem samples was performed in triplicate ( $n = 3$ ) using a Flash 2000 HT elemental micro-analyzer coupled to a thermal conductivity detector (TCD) (Thermo Scientific, Bremen, Germany). The calibration curve was made using acetanilide, nicotinamide, and aspartic acid as standard materials (Thermo Scientific, Bremen, Germany). The carbon isotope composition ratio (<sup>13</sup>C/<sup>12</sup>C) was determined by an elemental analyzer coupled to an isotope ratio mass spectrometer (EA/IRMS) using the protocols described by Miller et al. (2016, 2022). The EA/IRMS system (Thermo Scientific, Bremen, Germany) comprises a Flash 2000 HT analyzer with a combustion micro-reactor coupled to a Delta V Advantage isotope ratio mass spectrometer through a ConFlo IV interface. Stable isotope ratios are expressed as “ $\delta$ ” values referenced to the appropriate international standards and are reported in “per mil” (‰). Analytical precision (1 $\sigma$ ) of bulk  $\delta^{13}\text{C}$  was  $\pm 0.1$  ‰. Each replicate sample was measured in triplicate ( $n = 3$ ). The inorganic carbon was removed by sample digestion with a strong acid (HCl 1 M) before elemental and isotopic analysis.

Analytical pyrolysis (Py-GC/MS) was performed in a F-LAB Mod. 3030d double-shot microfurnace pyrolyzer (Frontier Laboratories, Koriyama, Japan) coupled to a gas chromatograph (Agilent 6890N). 10 mg of powdered and homogenized samples were weighed in crucible capsules and dropped in the pre-heated (500 °C) microfurnace for a minute. The evolved gases were directed to the chromatograph for separation using similar chromatographic conditions to those reported by Miller et al. (2022). The pyrolysis compounds were identified using a mass selective detector (Agilent 5973) in negative mode at 70 eV ionizing energy. Chemical structural information for each pyrolysis compound was achieved by analyzing their mass fragments and retention time and by comparison with published and stored mass libraries (NIST20 and Wiley7 libraries). The identified organic molecules released by Py-GC/MS were categorized into 8 organic families of known biogenic origin as described elsewhere (De la Rosa et al., 2019; Miller et al., 2022): aromatic compounds, polysaccharide-derived, peptides, lignin-derived, olefins, nitrogen compounds, polycyclic aromatic hydrocarbons (PAHs), and steranes. The relative abundance of the organic families was normalized according to the organic carbon content (%) previously determined by elemental analysis.

The organic compounds identified by Py-GC/MS were displayed as 3D van Krevelen plots as in Almendros et al. (2018) and Jiménez-Morillo et al. (2018). In brief, the empirical chemical formulas deduced from the mass spectra were used to calculate compound-specific O/C and H/C atomic ratios, which were then displayed in the x, y plane. On the other



hand, total abundances for individual compounds' chromatographic yields were determined and shown as the third dimension (z-axis).

## 2.6. Statistical analysis

Univariate (one-way analysis of variance, one-way ANOVA) and Principal Component Analysis (PCA) were performed using Statgraphics Centurion XVI.II software. PCA was used for simultaneous ordination of

different microbial communities at the order taxonomic level (higher than 0.5 % abundance), and the identified organic families obtained by analytical pyrolysis, illustrating established relationships.

The organic compounds identified by Py-GC/MS were displayed as 3D van Krevelen plots as in [Almendros et al. \(2018\)](#) and [Jiménez-Morillo et al. \(2018\)](#). In brief, the empirical chemical formulas deduced from the mass spectra were used to calculate compound-specific O/C and H/C atomic ratios, which were then displayed in the x, y plane. On the other

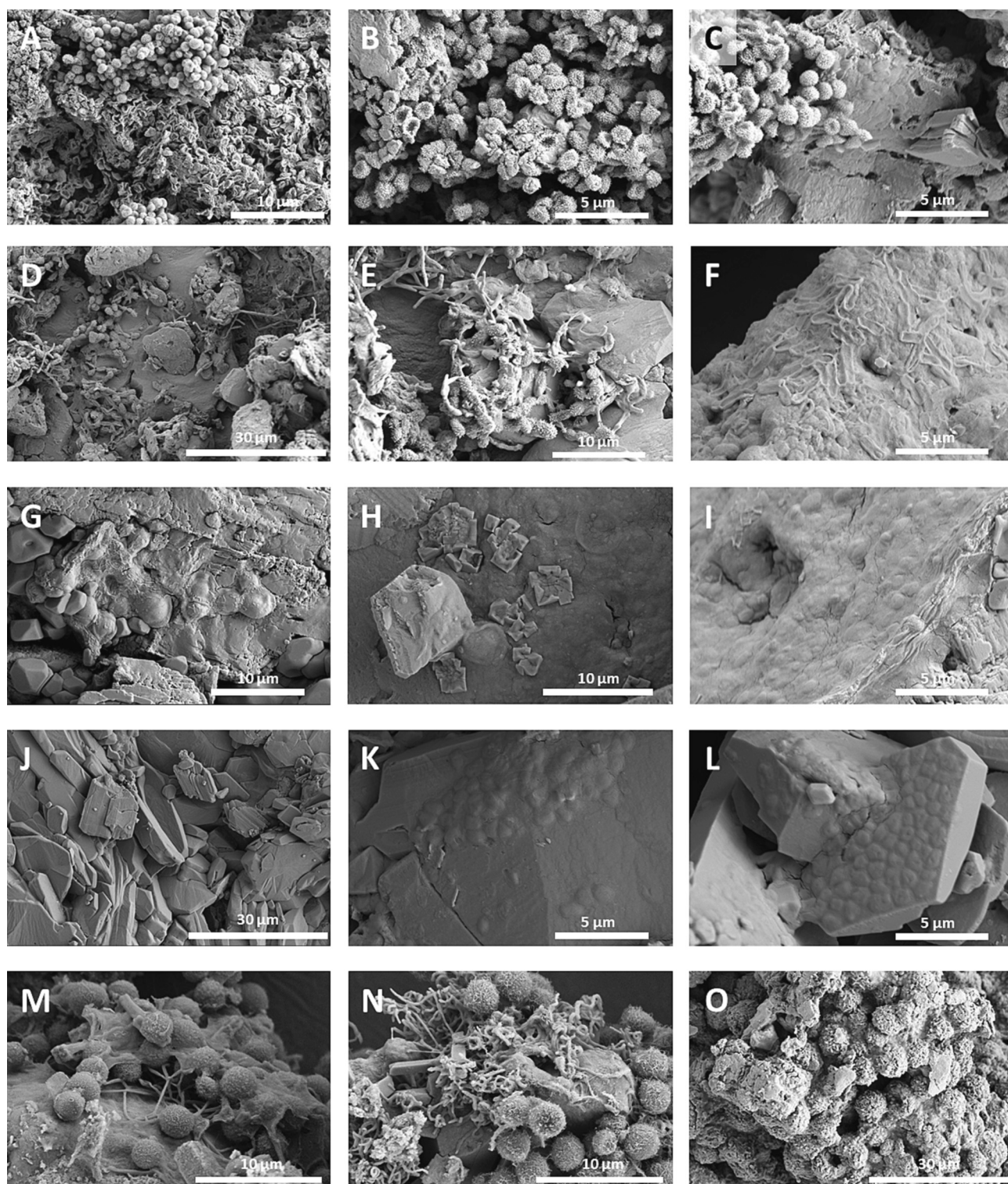


**Fig. 1.** Representative FESEM images of: samples CN1 (A–C) and CN2 (D–F) from *Cueva de los Naturalistas*; samples PE01 (G–I) and PE03 (J–L), *Paso Esqueleto* Cave; sample LB04 (M,N), *Cueva Las Breñas*, and sample MR02 (O) from *Montaña Rajada* Cave.

hand, total abundances for individual compounds' chromatographic yields were determined and shown as the third dimension (z-axis).

### 3. Results

#### 3.1. Morphological characteristics

Clear differences in microbial cell distribution and morphology were observed among samples imaged by FESEM (Fig. 1). Samples CN1 and CN2 from *Cueva de los Naturalistas* (CN) show a great abundance of actinobacteria-like cells, easy to identify by their characteristic spore chain ornamentation with surface appendages and hyphae-like structures resembling fungi. Sample CN1 shows dominance of coccoidal actinobacteria-like cell forms (<1 µm) with abundant surface appendages (Fig. 1A–C). A greater variety of microbial cell structures is observed in sample CN2, including coccoidal cells with spiny ornamentation, branched filaments, and rod-shaped cells with smooth surfaces (Fig. 1D–F), suggesting different microbial populations. Cell imprints on the mineral substrate associated with mineral dissolution features are also visible in sample CN1 (Fig. 1C), indicating microbe-mineral interactions.

In contrast, microbial cells are barely detected in samples from *Paso Esqueleto* Cave (PE), which mainly comprise coccoid-shaped cells impregnated in a matrix of extracellular polymeric substances (EPS) and in close association with mineral grains (Fig. 1G–L). The green biofilm sample PE01, collected in the twilight zone of the lava tube, shows collapsed coccoidal forms approximately 5 µm in size, which are consistent with photosynthetic-based microbial cells (Fig. 1G). These cells are in close association with salt crystals (Fig. 1H). In addition, bacterial cells, ~1 µm in size, appear embedded in a copious matrix of EPS (Fig. 1I). Sample PE03 depicts the characteristic habit of gypsum crystals (Fig. 1J), coated with biofilms of <1 µm coccoid-shaped cells that firmly adhere to mineral surfaces (Fig. 1K,L).

FESEM images from *Cueva Las Breñas* (LB04) reveal the presence of hairy Ca-rich spheroids 5 µm in diameter, closely associated with filamentous cells (Fig. 1M,N), resembling the CaCO<sub>3</sub> microspheres found in Kipuka Kanohina lava tube in Hawaii, USA (Riquelme et al., 2015) and the biogenic carbonate minerals associated with actinobacterial communities in *Altamira Cave* (Cuezva et al., 2012). Interestingly, the samples from *Montaña Rajada* (MR02) show an abundance of mineral grains embedded in EPS, forming spherical clusters of 5–10 µm in diameter (Fig. 1O), suggesting a biomineralization process where EPS may serve as nucleation sites for mineral precipitation.

#### 3.2. Mineralogical composition

The analysis of secondary minerals collected in the four lava tubes shows that sulfates, carbonates, and amorphous silica prevail (Table S1). Samples from *Cueva de los Naturalistas* are constituted by fragments of the basaltic host rock (silicate minerals of the olivine, pyroxene, and plagioclase groups) with minor amounts of secondary calcite and gypsum. Sample CN2 exhibits an important amount of amorphous phase, depicted as a distinctive bulge in the XRD spectra. The crust collected from *Montaña Rajada* (MR02) consists almost entirely of gypsum. Both samples from *Paso Esqueleto* are gypsum with minor halite, whereas the one from *Las Breñas* (LB04) is made up of authigenic fluorapatite.

#### 3.3. Taxonomic composition and distribution of prokaryotic communities

A total of 314,917 paired-end sequences were obtained by 16S rRNA gene sequencing after quality trimming and denoising all samples, yielding 1711 ASVs at a 97 % similarity threshold (Table 2). The microbial communities of the analyzed samples are almost entirely composed of *Bacteria*, with a minor presence of *Archaea*, ranging between 0.412 % and 0 %, for MR02 and LB04 samples, respectively. DNA samples failed to yield positive PCR results using the primer pairs ITS1/

**Table 2**

Alpha diversity estimation by sample using Shannon diversity and Pielou's evenness metrics.

	Feature count	Observed ASVs	Shannon	Pielou
PE01	66,955	340	5.021024	0.5970734
PE03	49,020	164	4.707333	0.6397961
CN1	52,966	259	3.225700	0.4023671
CN2	44,735	614	6.723265	0.7258903
LB04	55,859	78	1.876880	0.2986093
MR02	45,382	256	4.705176	0.5881470

ITS4 and 109F/915R for fungi and archaea, respectively, probably due to the low abundance of these microorganisms in the samples or primer specificity.

Bacterial communities show heterogeneity in composition (Fig. 2), with the *Bacillota*, *Actinomycetota*, and *Bacteroidota* phyla as the most abundant, exceeding 50 % for most of the sampling sites. *Bacillota* is the most abundant phylum in samples MR02 and PE01, with 90.5 % and 85.2 % of representativeness, respectively. Albeit they were collected in different lava tubes, both samples comprise green photosynthetic-based biofilms on white secondary gypsum deposits and show similarities in microbial diversity. *Actinomycetota* exceeds 90 % of abundance in sample LB04, 66.7 % in CN1, and 47.3 % in CN2, whereas *Bacteroidetes* show 81.1 % of representativeness in PE03.

Less abundant phyla are *Pseudomonadota*, *Chloroflexota*, *Cyanobacteriota*, and *Gemmatimonadota*, exceeding 5 % of representativeness in at least one of the samples. *Pseudomonadota* is present in all samples but with a significant abundance above 5 % in PE01, CN2, and LB04 (Fig. 2). Members of the phylum *Chloroflexota* exist in CN1 and CN2, exceeding 12 % of abundance, whereas *Gemmatimonadota* was mostly found in CN2 with >5 %. *Cyanobacteriota* in PE01 and MR02 account for 3.7 % and 2.6 %, respectively.

At lower taxonomic levels, both MR02 and PE01 show a high abundance of the genus *Clostridium* sensu stricto, exceeding 53 % and 49 %, respectively. In contrast, one uncultured genus within the family *Euzeyaceae* was identified in sample CN1 (>58 % of abundance), whereas, in LB04, the genus *Crossiella* is the most significant group, with 74.3 % of representativeness (Fig. 2). *Actinomycetota* is also the dominant phylum in sample CN2. It is worth mentioning that one unassigned order within the class *Acidimicrobiia* was found in CN2 with 15.4 % of abundance, followed by the genus *Rubrobacter* (8 %). This uncultured genus belonging to the family *Euzeyaceae*, was also identified in sample CN1. The genus *Pseudonocardia* and the order *Frankiales* are less significant, with 4.2 % and 3.3 %, respectively. The most abundant group (76.4 % of representativeness) in sample PE03 is the family *Balneolaceae* (Fig. 2).

Richness and evenness of microbial communities were estimated by Shannon diversity and Pielou's evenness indices, which are reported in Table 2. We generated a total of 1711 ASVs, ranging between 614 and 78 for samples CN2 and LB04, respectively. CN2 was determined as the most biodiverse sample with the highest species richness, with Shannon and Pielou's evenness indices of 6.723 and 0.725, respectively. In contrast, sample LB04 was the least diverse, with 78 observed ASVs and Shannon and Pielou indices of 1.876 and 0.298, respectively, followed by sample PE03.

The relationship between the microbial communities among samples measured using the metric UniFrac shows differential divergences in its variation unweighted after calculating the fraction of the branch length in the phylogenetic tree generated for the analyzed samples, in special regarding sample LB04 (Fig. S2). CN1 and CN2 were relatively close to each other, as well as PE01 and MR02, which seem to share a close relationship, possibly due to their location in the twilight zone of the respective lava tubes. The variation weighted UniFrac reinforces the distribution and relatedness of the abundance in the bacterial communities observed in the taxonomic analyses, grouping the samples according to the abundance of different phyla (*Actinomycetota*: CN1, CN2,



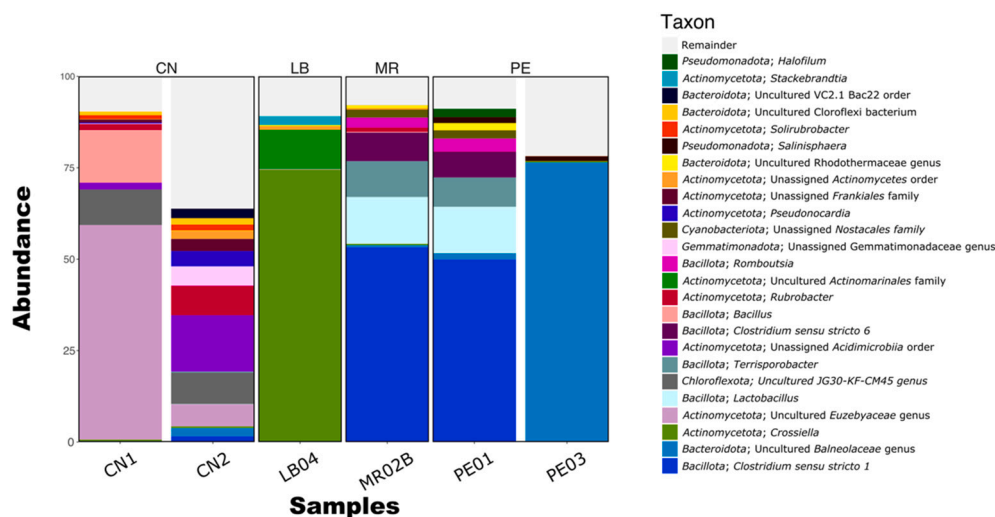


**Fig. 2.** Taxonomic distribution (%) in “Cueva de los Naturalistas” (CN), “Paso Esqueleto” (PE), “Montaña Rajada” (MR), and “Las Breñas” (LB), retrieved from High-throughput sequencing of DNA at phylum and lower taxonomic levels. Within “Remainder” are included all the groups with <1 % of representativeness (<1 % of total).

and LB04; *Bacillota*: PE01 and MR02; *Bacteroidota*: PE03). PERMANOVA did not present statistically significant differences among samples regardless of the used variations (unweighted,  $P = 0.144$ ; weighted,  $P = 0.336$ ).

The functional profile of microbial communities predicted by PIC-RUST2 shows inter-sample variations as well as similarities providing relevant insights into biological processes in the microbial communities (Fig. 3). Methane metabolism did not achieve a relevant role in any of the analyzed samples. The gene that encodes the factor 420-reducing hydrogenase was solely represented by 27 % of microorganisms in sample CN2. This enzyme participates in the first step of the methanogenesis process carried out by some archaea. However, this enzyme is relevant in anaerobic metabolism, catalyzing the oxidation of molecular hydrogen using  $\text{Ni}^{2+}$  as cofactor. Other taxa found in sample CN2 had an abundance below 10 % and included *Actinomycetota* members, such as *Pseudonocardia* and *Frankiales*, as well as *Chloroflexota*, *Bacillota*, *Bacteroidota* or *Gemmatimonadota* with diverse trophic roles.

Sulfur metabolism appears to be relevant in samples CN1, CN2, PE03, and LB04, having low incidence in PE01 and MR02 (Fig. 3). The genes encoding the enzymes adenylyl-sulfate reductase, sulfate adenylyltransferase, and phosphoadenylyl-sulfate reductase (NADPH) are part of the assimilatory sulfate reduction pathway, where the sulfate is reduced to sulfite.

Regarding the characterized genes involved in the  $\text{CO}_2$  fixation, three groups with high abundance were differentiated. One is formed by those that encode the enzymes fumarate reductase (quinol), 2-oxoglutarate synthase, 2-oxoacid oxidoreductase (ferredoxin), and pyruvate synthase, which participate in reductive TCA cycles, where the  $\text{CO}_2$  fixation is carried out. The second group comprises those genes for the proteins Acetyl-CoA carboxylase and biotin carboxylase involved in the carboxylation of biotin to form malonyl-CoA using  $\text{CO}_2$ . The third group includes the genes encoding the enzymes phosphoenolpyruvate carboxylase and carbonate dehydratase, which produce the fixation of  $\text{CO}_2$  into oxaloacetate.

The functional group involved in nitrogen metabolism was also relevant. The genes encoding the ammonia assimilation enzymes, including glutamate synthase, glutamate dehydrogenase, and glutamate-ammonia ligase, stand out in the nitrogen metabolism for all samples (Fig. 3). The genes for the proteins nitrate reductase and nitrite reductase (NADH), which convert nitrate to nitrite and nitrite to ammonia, respectively, are highly abundant in sample LB04. Similarly, the genes encoding the enzyme urease, involved in the formation of

ammonia and  $\text{CO}_2$ , are noticeable in this sample. For PE03, the gene encoding the protein nitrite reductase (NO-forming) shows the highest abundance. This enzyme participates in the transformation of ammonia to  $\text{N}_2$  in the denitrification pathway. MR02 and PE01 show metabolic similarities that differentiate them from the rest of the samples. Worth noting is the presence of genes encoding the enzymes ferredoxin—nitrite reductase (assimilatory), hydroxylamine reductase, and carbamate reductase, involved in the reduction of nitrite, the reduction of hydroxylamine and the hydrolysis of carbamate to ammonia.

### 3.4. Bacterial isolates

A total of 22 isolates were identified from three out of six cave samples (PE01, MR02, and LB04). The identified phyla comprise *Bacillota*, *Actinomycetota*, *Pseudomonadota*, and *Bacteroidota* (Table S3). The phylum *Bacillota* is the most abundant in samples PE01 and MR02, with 100 % and 75 %, respectively, whereas *Actinomycetota* is the most abundant phylum in sample LB04, representing 71.43 %. This is in fair agreement with the metagenomic analysis (Fig. 2).

The 16S rRNA gene sequence of the two strains isolated from MR2 and PE01 only have 94.65 % and 93.75 % of similarity, respectively, to the species on the database: *Virgibacillus phasianinus* (belonging to *Bacillota*) and *Nafulsella turpanensis* (*Bacteroidota* phylum). This indicates that these strains are potential new bacterial species (Kim et al., 2012; Rosselló-Mora and Amann, 2001; Stackebrandt, 2003).

### 3.5. Isotopic and molecular composition

The total organic carbon content shows a mean value of 0.35 % (Table 3), indicating a low abundance of OM preserved in speleothems. The only exception is sample CN1, which shows a significantly high TOC value (8.38 %) but a far more positive  $\delta^{13}\text{C}$  value.

The  $\delta^{13}\text{C}$  values of the speleothem samples (not including CN1) range from  $-32.0$  ‰ to  $-21.5$  ‰, values that are typical of  $\text{C}_3$  photosystem vegetation (Fry, 2006; Miller et al., 2016, 2020a). However, there are significant differences among samples, as revealed by one-way ANOVA (Table 3). The lowest  $\delta^{13}\text{C}$  values ( $-32.0$  ‰ and  $-29.8$  ‰) occur in samples CN2 and PE01, respectively. The PE03, MR02, and LB04 show an organic fraction with the highest proportion of heavy C isotope ( $-21.5$ ,  $-25.5$ , and  $-23.5$  ‰, respectively) (Table 3).

The molecular composition of the organic fraction preserved in the speleothems is depicted as 3D van Krevelen diagrams (Fig. 4). This

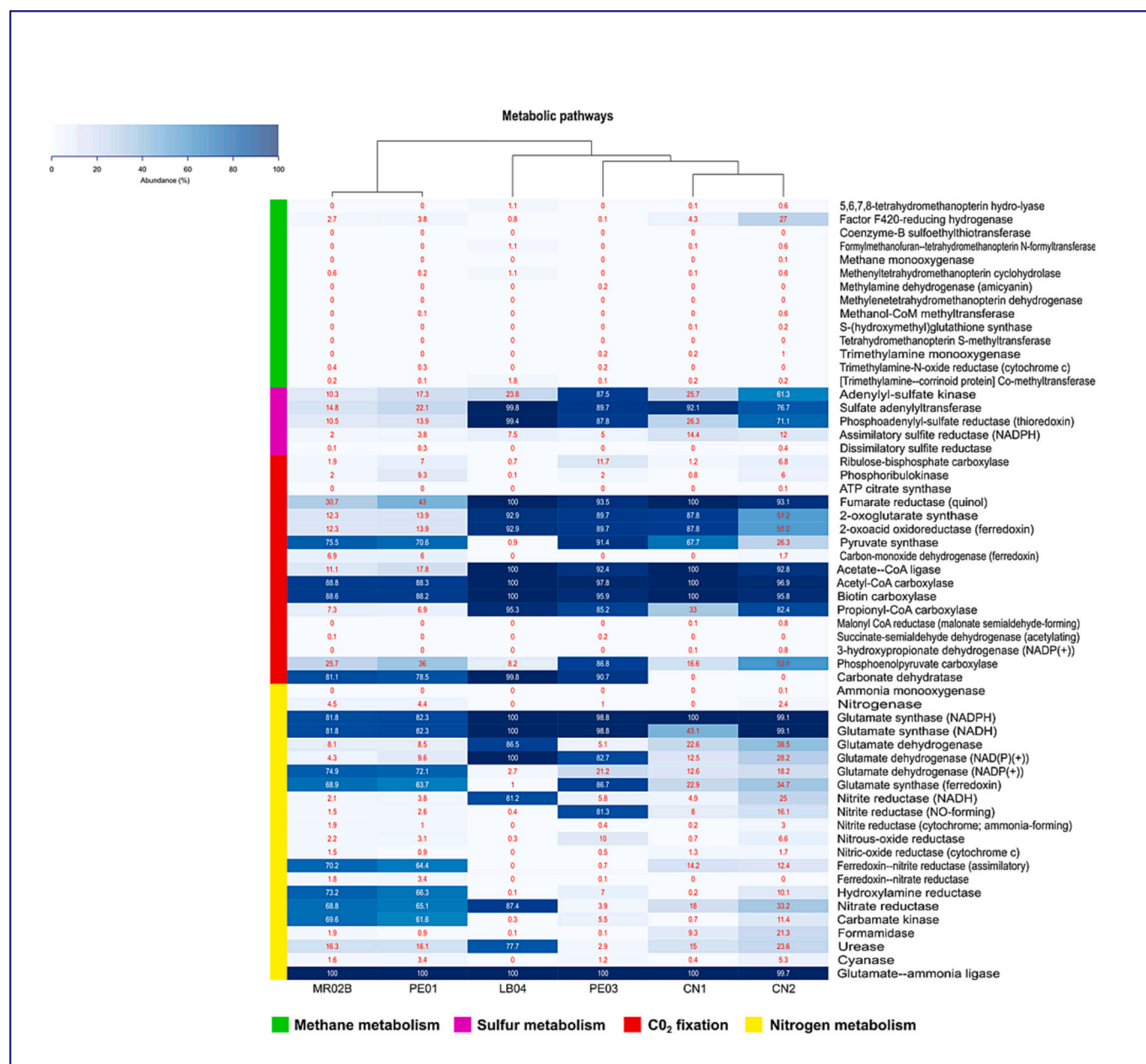


**Fig. 3.** Heatmap showing the relative abundance of PICRUSt2 predicted genes encoding the enzymes involved in methane, sulfur, CO<sub>2</sub> fixation, and nitrogen metabolism.

**Table 3**

Mean ( $\pm$ standard deviation) bulk isotopic carbon signature ( $\delta^{13}\text{C}$ ) and total organic carbon (TOC) of the selected samples from Lanzarote lava tubes.

Sample ID	$\delta^{13}\text{C}$ (‰, VPDB)	TOC (%)
CN1	$-9.6 \pm 0.50^c$	$8.38 \pm 0.20^d$
CN2	$-32.0 \pm 0.90^a$	$0.42 \pm 0.02^b$
PE01	$-29.8 \pm 0.00^a$	$0.18 \pm 0.00^a$
PE03	$-21.5 \pm 0.10^b$	$0.18 \pm 0.01^a$
MR02	$-25.5 \pm 0.40^b$	$0.83 \pm 0.06^c$
LB04	$-23.5 \pm 3.80^b$	$0.13 \pm 0.02^a$

Different letters indicate significant differences ( $P < 0.05$ ) between compounds according to the Tukey test.

graphical statistical method allowed identifying the major organic families within the pyrochromatograms of each lava tube. Sample CN1 is dominated by aromatic, peptide and lipid-like compounds (Fig. 4A).

This latter family is composed of a mixture of cyclized lipids (e.g., cyclohexane, 1-(1,1-dimethylethyl)-4 methyl), *n*-alkane/alkene pairs, oxygenated alkyl compounds (e.g., 2-isononanal), as well as a few saturated and unsaturated alkanolic acids (e.g., palmitoleic acid, stearic acid; Table S4). In addition, branched unsaturated alkanolic acid (3,7,11-Trimethyl-dodeca-2,6,10-trienoic acid), which is one of the major components of bacterial membranes (Kaneda, 1991), is also present in sample CN1. Regarding aromatic and peptide-derived compounds, molecules of pyridine and indole are the main constituents (Table S4). Another remarkable aspect is the high abundance of lignin-derived compounds, including methyl-phenols. The presence of furan compounds (such as 3-furaldehyde and 2-furancarboxaldehyde, 5-methyl) is also observed in CN1 and CN2 (Fig. 4A,B and Table S4). The 3D van Krevelen diagram of sample CN2 also shows a relatively high contribution of peptide and aromatic compounds, and lipids (mainly short-chain *n*-alkane/alkene pairs).



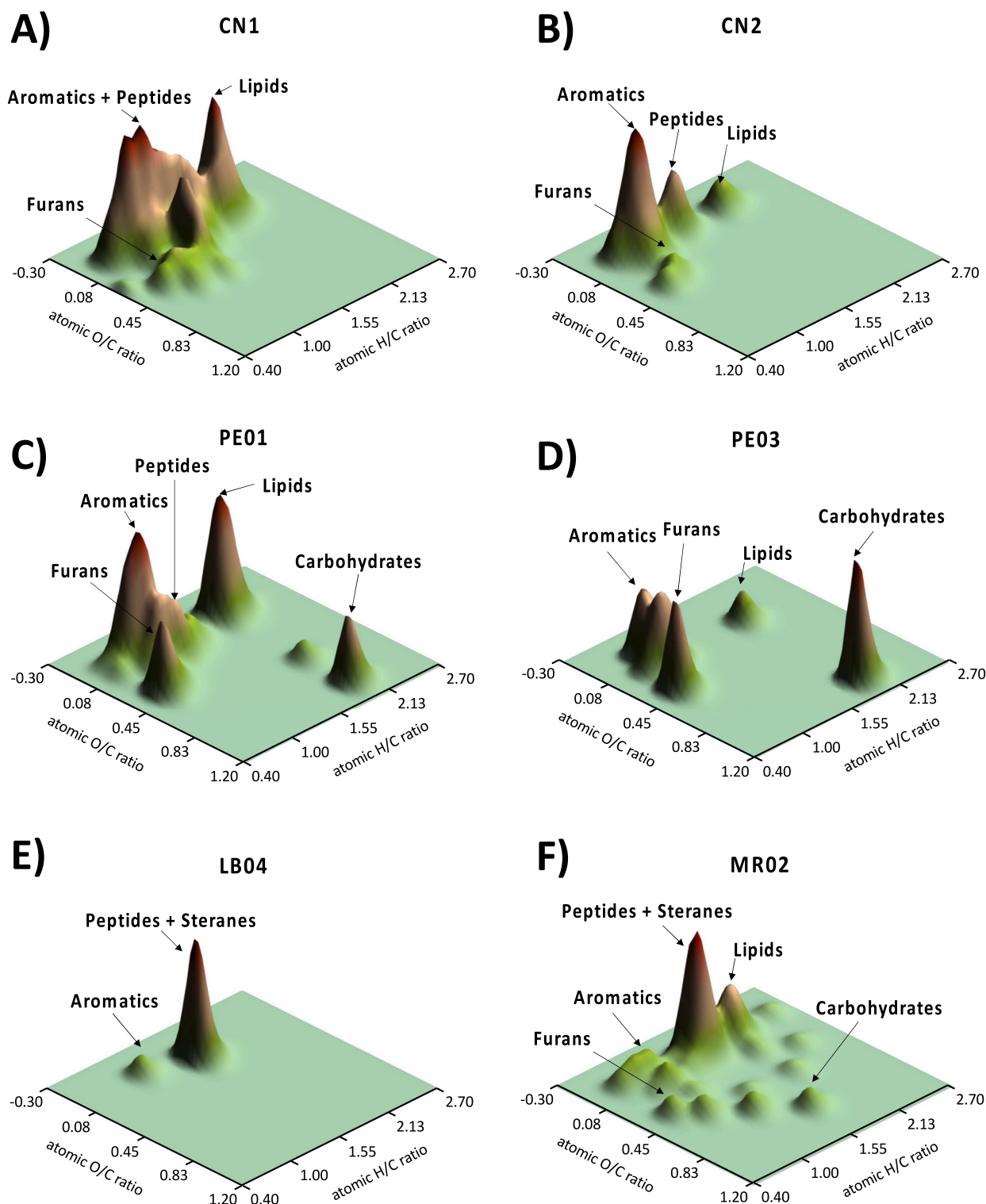


**Fig. 4.** 3D van Krevelen diagrams of the cumulative abundances of pyrolysis products plotted in the space defined by the H/C and O/C atomic ratios for each cave sample: A) CN1; B) CN2; C) PE01; D) PE03; E) LB04, and F) MR02. Labels on the plots indicate major organic families.

The PE01 and PE03 speleothems show similar organic composition but with different relative abundances. The PE01 is clearly dominated by lipids and aromatics (Fig. 4C) with a clear contribution of carbohydrates (polysaccharides and furans). In contrast to CN, the peptide and N-containing compounds are almost completely absent in PE samples (Table S4). A detailed integration of the pyrochromatogram from PE01 reveals that the lipid fraction is composed of short and medium-chain *n*-alkane/alkene pairs ( $C_{11}$ - $C_{19}$ ) with the presence of some *n*-alkanoic acids

(Table S5). In addition, Neophytadiene, a branched unsaturated alkene derived from isoprene, is detected in PE01 (Table S4). Carbohydrates and furans are the main families, followed by aromatics observed in PE03 (Fig. 4D).

The LB04 is clearly dominated by two peaks identified as steranes (Fig. 4E). In addition, this sample depicts the presence of peptides and aromatics (benzenes and alkyl-benzenes) and a relatively low abundance of a series of short/medium-chain *n*-alkane/alkene pairs (lipids;

Tables S4 and S5).

The MR02 contains a highly diverse organic fraction, with a remarkable presence of peptide, steranes and lipids (Fig. 4F; Table S4). The lipid fraction is composed of branched compounds, such as Phytane, Phytene, 13-methyl- $\alpha$ -14-nonacosene (Table S4). This sample also shows molecules of carbohydrates, aromatics, peptides, and steranes (e.g., 17-androstanone,  $\alpha$ -amyrin; Table S4).

The relative abundance of the lipid-like compounds released by Py-GC/MS (Table S5) is shown in Fig. 5. Sample MR02 depicts the highest molecular diversity, while LB04 solely shows *n*-alkanes/alkenes pairs. CN1 does not present alkane compounds (linear and branched), while the lipidic fraction of CN2 is only composed of *n*-alkanes,  $\alpha$ -alkenes, and other lipids (e.g., aldehydes). Speleothems PE01 and PE03 show remarkable differences. The lipid fraction of PE01 is mainly composed of *n*-alkane/alkene pairs, and lipids (e.g., alcohols, terpenes, and aldehydes; Table S5). In contrast, PE03 shows a relatively high abundance of  $\alpha$ -alkenes, *n*-alkanoic acids, and aldehyde-like compounds. Branched alkanoic acids were only detected in samples CN1 and MR02.

### 3.6. Relationships among microbial diversity, organic matter, and mineralogical composition

Principal component analysis was computed to assess and understand the statistical relationship among microbial diversity (dependent variable), main organic families preserved in speleothems, and the mineralogical composition of secondary mineral deposits (independent variables) documented in the lava tubes. The first two components explained 65 % of the variation observed (Fig. 6). The score plot of PC-1 vs PC-2 defines three clusters (Fig. 6A), sorting the lava tube samples based on the most abundant bacterial orders, organic matter, and type of minerals. Samples from *Cueva de los Naturalistas* (CN1 and CN2) define cluster-I, whereas *Cueva de Las Breñas* sample (LB04) groups in cluster-II. Cluster-III includes the samples from *Paso Esqueleto* (PE) and *Montaña Rajada* (MR02), showing no significant differences in bacterial community composition and organic families in both lava tubes.

The scatterplot of the loadings of PC-1 vs PC-2 also defines three clusters (Fig. 6B). Cluster-I shows a heterogeneous group of microorganisms from CN, mainly composed of bacteria belonging to the phyla *Actinomycetota* (orders *Euzebyales*, *Rubrobacterales*, *Solirubrobacterales* and *Frankiales*), followed by *Gemmatimonadota* (order *Gemmatimonadales*), *Chloroflexota* (order *Thermomicrobiales*), *Pseudomonadota* (order *Sphingomonadales*), and *Bacillota* (order *Bacillales*). These directly

correlate to the presence of PAHs, peptides, nitrogen compounds (N comp), and lignin. Furthermore, these microbial orders correlate strongly with the presence of calcite ( $\text{CaCO}_3$ ) and anorthite ( $\text{CaAl}_2\text{Si}_2\text{O}_8$ ). In contrast, cluster-II shows a well-differentiated homogenous group of microbial taxa, dominated by members ascribed to the *Actinomycetota* phylum (orders *Pseudonocardiales*, *Micromonosporales*, and *Actinomariniales*; Fig. 6B), which are associated with ilmenite ( $\text{FeTiO}_3$ ), forsterite ( $\text{Mg}_2\text{SiO}_4$ ), nepheline ( $\text{Na}_3\text{KAl}_4\text{Si}_4\text{O}_{16}$ ), and fluorapatite ( $\text{Ca}_5(\text{PO}_4)_3\text{F}$ ), as well as sterane compounds. The phylotypes belong mainly to the phyla *Pseudomonadota* (orders *Nevskiales* and *Chromatiales*) and *Bacillota* (orders *Eubacteriales* and *Lactobacillales*), as well as the orders *Bacteroidales*, *Balneolales*, *Rhodothermales*, and *Nostocales* (cluster-III) link to aromatic and lipid compounds, which are primarily related to clinopyroxene ( $(\text{Ca,Mg,Fe,Na})(\text{Mg,Fe,Al})(\text{Si,Al})_2\text{O}_6$ ), halite ( $\text{NaCl}$ ), and gypsum.

## 4. Discussion

The secondary minerals identified in this study fall into two groups: one comprises minerals directly precipitated from sea spray salts, such as gypsum and halite, forming crusts and efflorescences near entrances, especially in lava tubes close to the sea, such as PE and MR lava tubes. The second group (calcite, gypsum, and opal), results from the interaction between seepage water and volcanic bedrock, and occur as crystalline and fibrous crusts, powdery deposits, and coralloids in more remote parts of lava tubes (Fig. 7). Calcium in calcite, gypsum, and fluorapatite originates from percolating waters dissolving minerals in basalts (e.g., anorthite), while sulfate may come from volcanic gases or the oxidation of sulfide minerals. Opal-AG (Amorphous-Gel), a subtype of opal-A, is XRD amorphous and likely the mineral present in the CN2 sample. It resembles forms found in orthoquartzite caves (Sauro et al., 2018), with silicon sourced from silicate mineral weathering. The identified gypsum and opal in this study share similarities with those on Mars, observed in the Endeavor and Gusev craters (Squyres et al., 2008; Rice et al., 2010).

Microbial communities characteristic of oligotrophic environments have been documented in speleothems formed in lava tubes (Fishman et al., 2023; Northup et al., 2011; Teehera et al., 2018). If similar speleothems exist in lava tubes on Mars, microbes could be leveraging the inter- and intra-granular spaces within secondary minerals as microenvironments in which to grow and further mediate mineral precipitation.

The bacterial communities of Lanzarote lava tubes are predominantly composed of chemoorganotrophic, halophiles, and/or

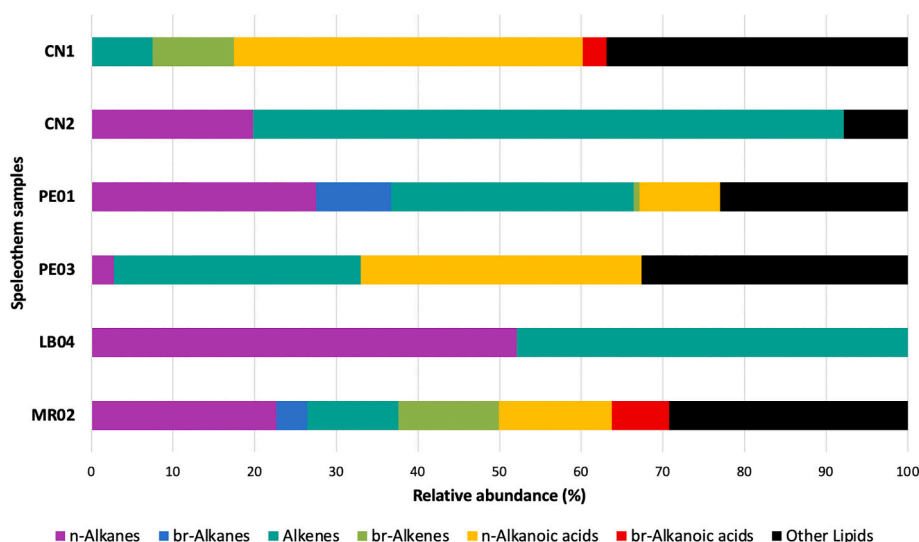
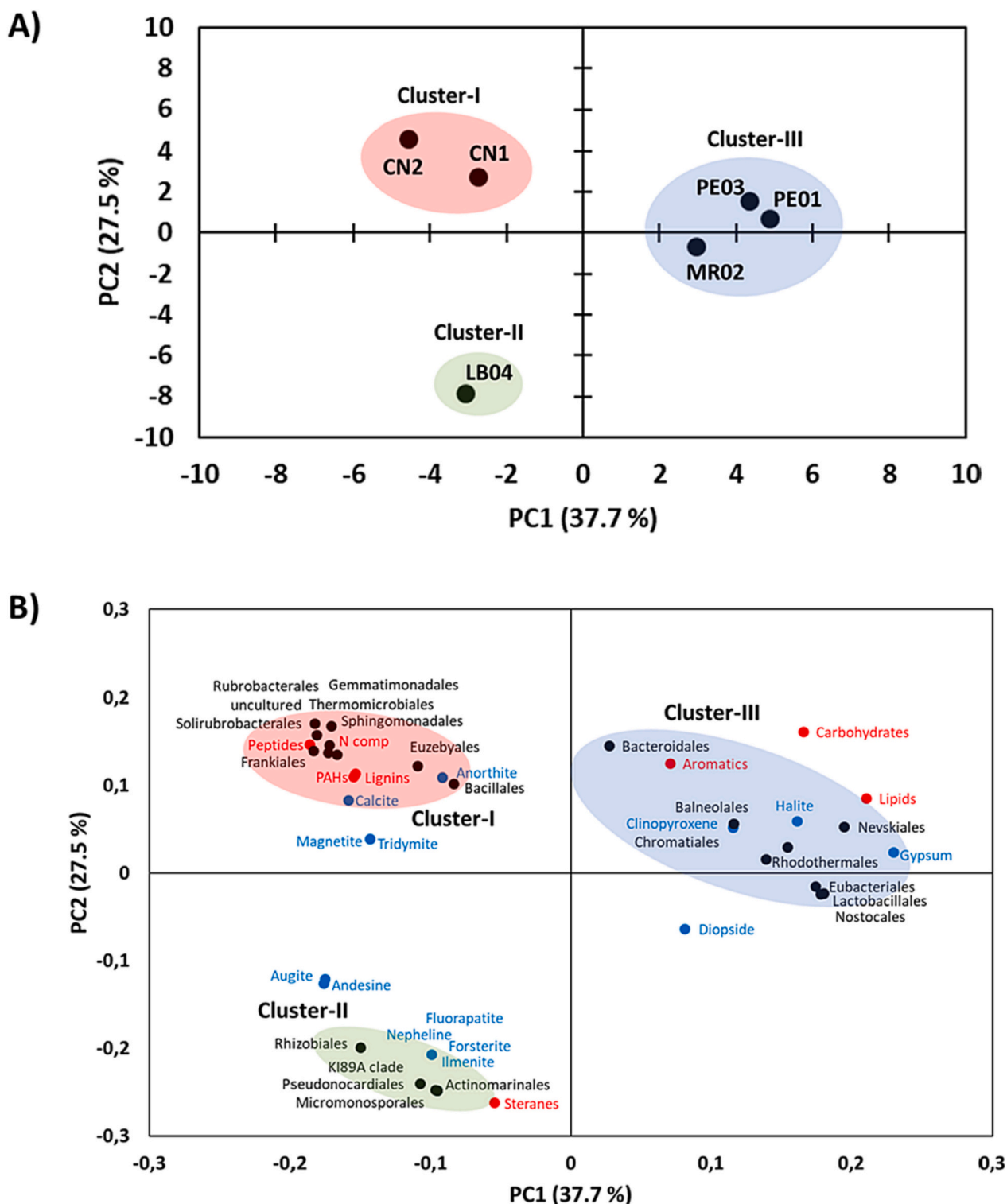


Fig. 5. Relative abundance of the main lipid-derived compounds identified by analytical pyrolysis.



**Fig. 6.** Principal components analysis of the six sampling sites studied from four Lanzarote lava tubes. (A) Score plot of the speleothem samples. (B) Plot of loading weights for the organic families identified by Py-GC/MS (red labels), the mineralogical composition (blue labels), and the most abundant taxa at the order level (black labels).

halotolerant bacteria. These microorganisms have evolved in response to the surrounding oceanic conditions, particularly sea spray inside the caves. Within chemoorganotrophy, *Clostridium*-related bacteria were identified near the cave entrances, such as *C. celatum* and *C. butyricum*. These anaerobic Gram-positive bacteria are commonly found in guano, and animal and human digestive tracts (Hauschild and Holdeman, 1974; Rainey et al., 2009). The high incidence of this genus in PE01 and MR02

could be due to the nesting of seagulls and *Calonectris diomedea* close to the cave entrances, where abundant guano was observed adjacent to the sampling sites in both caves. This, along with the sunlight entering caves, explains the predominance of *Clostridium* and the presence of photosynthetic-based biofilms on the cave walls. The functional profile of microbial communities from PE01 and MR02 is closely related, agreeing with the observed sample relatedness using the unweighted



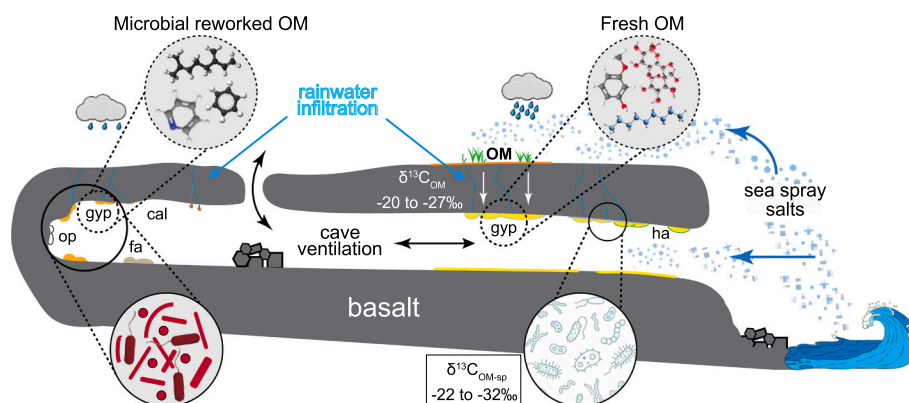


**Fig. 7.** Conceptual diagram showing different environments under which secondary minerals precipitate in lava tube (cal: calcite, fa: fluorapatite, gyp: gypsum, ha: halite, op: opal) and their associated microbial assemblages.

UniFrac calculation (Fig. S2).

In LB04 from *Cueva Las Breñas*, the genus *Crossiella* holds particular importance, given that only two species affiliated to this group have been described previously: *C. equi*, extracted from equine placentas (Donahue et al., 2002), and *C. cryophile*, originally isolated from soils (Labeda, 2001). *Crossiella* has been reported in lava tubes and karstic caves associated with weathered rocks and speleothems (Gonzalez-Pimentel et al., 2021; Ma et al., 2021; Miller et al., 2020b; Nicolosi et al., 2023). Interestingly, *Crossiella* has been suggested to play a role in  $\text{CaCO}_3$  precipitation via urea hydrolysis in deteriorated cultural heritage (Li et al., 2018). The presence and relative abundance of genes encoding the urease enzyme (EC:3.5.1.5) in LB04 suggest its involvement in mineral precipitation, potentially of fluorapatite, in *Las Breñas* lava tube. This hypothesis is supported by the Ca-rich biogenic-like mineral grains observed by FESEM (Fig. 1M,N), and the mineralogical composition of the white microbial mats observed in *Las Breñas* (Table S1). Riquelme et al. (2015) described similar carbonate microspheres closely related to actinobacteria in a lava tube from Azores, Portugal. Koning et al. (2022) and Martin-Pozas et al. (2023) demonstrated the involvement of urease-positive bacteria, particularly *Crossiella*, in forming speleothems. The available data strongly suggest the likelihood of biologically mediated precipitation of Ca-rich microspheres and potentially of fluorapatite by *Crossiella*. Fluorapatite produced by bacteria with carbonatogenic ability has been reported in Colombian mines (García et al., 2016). These carbonate-rich minerals may leave behind an organic record that remain more or less unchanged for millions of years, providing evidence of past or present life (Blyth and Frisia, 2008; Westall et al., 2015; Chan et al., 2019; Kosznik-Kwaśnicka et al., 2022). The Ca-rich microspheres formed by the activity of *Crossiella* are proposed here as compelling biosignatures for astrobiology. Thus, speleothems serve as crucial repositories for extant and past microbial life, representing a unique setting to search for biosignatures (Wynne et al., 2022).

Halophiles or halotolerant bacterial communities closely related to marine and other salty environments were also identified in Lanzarote lava tubes. This is the case of the uncultured genus affiliated to the *Balneolaceae* family present in PE03 from *Cueva Paso Esqueleto*, exceeding 76 % of representativeness. As revealed by XRD, PE03 is mainly composed of gypsum (94 %), a secondary mineral occurring in numerous caves and lava tubes around the world (Forti, 2005; Onac and Forti, 2011). Huerta et al. (2019) argue that gypsum speleothems in Lanzarote precipitated due to the evaporation of sea spray penetrating deep inside lava tubes or from remobilization of surface gypsum (also from sea spray) by percolating water. Such speleothems formed due to sea spray could act as suitable niches for *Balneolaceae* members, which were originally isolated from seawater or salt mines (Xia et al., 2016).

The *Euzebyaceae* family, identified as the most abundant taxon in CN1 and also observed in CN2 from *Cueva de los Naturalistas*, is a group

associated with sea environments. This family solely includes one genus, *Euzebya*, with three species affiliated to this group: *E. tangerina*, *E. rosea*, and *E. pacifica* (Jian et al., 2021; Kurahashi et al., 2010; Yin et al., 2018). The *Euzebyaceae* family has been previously observed in lava tubes located on oceanic islands, such as the Canary, Hawaii, and Galapagos (Gonzalez-Pimentel et al., 2018, 2021; Miller et al., 2020b; Riquelme et al., 2015), as well as in karstic caves, making it a ubiquitous group in underground environments (Cuezva et al., 2012; Velikonja et al., 2014).

The microbial diversity of the samples was consistent with the metabolic pathway patterns predicted (Figs. 3 and 4). Samples showing similar microbial composition have similar metabolic patterns, also supported by PCoA analysis (Fig. S2). Sample CN2 depicts the highest microbial diversity and even distribution, whereas PE03 and LB04 display the lowest microbial diversity. Our study indicates that similar environmental conditions lead to the establishment of identical microbial compositions regardless of the geographic location on the same island, i.e., MR02 and PE01. On the other hand, LB04 and PE03 seem to have unique characteristics that drive the settlement of distinct bacterial communities.

Generally, the bacterial isolates from Lanzarote lava tubes are also dominated by halophilic bacteria associated with marine environments, corroborating amplicon metagenomics data. Most bacterial strains were first isolated from seawater, marine sediments, or marine organisms like sponges or anemones (Table S3). In PE01, all isolates fall under the phylum *Bacillota*. Within this phylum, two strains of the species *Staphylococcus warneri* were identified. This species has been previously isolated from the cloaca of Arctic terns (*Sterna paradisaea*), a migratory bird that winters in the South Atlantic. It shares its migration route with other birds, like Cory's shearwater (*Calonectris diomedea*) that nests in the vicinity of *Cueva Paso Esqueleto* (Prakash et al., 2022). This bacterium is also capable of inducing precipitation of carbonate minerals at various Mg/Ca molar ratios (Han et al., 2020). Another species isolated in PE01 was *Sporosarcina newyorkensis*, which can catalyze the precipitation of calcium carbonate by urea hydrolysis (Hata et al., 2020).

In MR02, the strain *Mesobacillus campisalis*, belonging to the phylum *Bacillota*, shows the ability to induce the precipitation of calcium carbonate (Idris et al., 2022), while the halophilic *Pseudobacteriota* strain *Halomonas xianhensis* exhibits an efficient production of EPS (Biswas et al., 2015). This is consistent with the FESEM images showing minerals embedded in EPS.

The C isotope analysis of the speleothems from Lanzarote lava tubes reveal the direct influence of the overlying layers (mostly weathered basaltic pyroclasts) and vegetation in the formation of the speleothems, as also documented in other lava tubes (Miller et al., 2016, 2020a, 2022). Samples CN2 and PE01 show the lowest  $\delta^{13}\text{C}$  values, indicating inputs from plants of the surface layers or contributions from specialized microorganisms, like methanogenic archaea (Boschker and Middelburg,

2002). Biogenic methane ( $\text{CH}_4$ ) produced by these archaea is known to be  $^{13}\text{C}$ -depleted (Whiticar, 1999). The relatively high presence (27 %) of the gene encoding the enzyme 420-reducing hydrogenase in CN2 supports the hypothesis of microbial methanogenesis, which results in low  $\delta^{13}\text{C}$  organic compounds (Fiebig and Friedrich, 1989). For the photosynthetic-based biofilms on secondary gypsum deposits (PE01), the DNA-based analysis showed the presence of cyanobacteria (3.7 %, Fig. 2), which may produce the same isotopic signature as  $\text{C}_3$  plants (Hayes, 2018). The samples PE03, MR02, and LB04 show the highest proportion of heavy C isotope, which may be attributed to microbial reworking of organic materials (Fig. 7), as observed by Miller et al. (2022) in Galapagos lava tubes.

The combination of molecular data, obtained by analytical pyrolysis (Py-GC/MS), and graphic-statistical tools allow visualizing and comparing the organic families of the complex organic fraction preserved in Lanzarote lava tubes (Fig. 4). Samples PE01 and PE03 show the predominance of lipids, polysaccharides, and furans, which may derive from EPS, clearly observed by FESEM (Fig. 11). The lipid fraction of PE01 and PE03, mainly consisting of i) low-chain *n*-alkane/alkene pairs and branched alkenes, and ii) short chain C length  $\alpha$ -alkenes and *n*-alkanoic acids (Table S5), respectively, further supports the microbial origin of organic matter in these speleothems (Blyth et al., 2008, 2011). The short-chain aliphatic compounds are characteristic of the cellular membrane of microorganisms (Hashimoto and Hossain, 2018) and/or microbial activity (Jiménez-Morillo et al., 2017, 2020). In PE01, the microbial origin of the organic fraction may be also supported by the presence of neophytadiene (isoprene). This branched alkene is frequently associated with eukaryotic microorganisms and archaea, as they use isoprene compounds as a precursor of the cellular membrane (Jain et al., 2014; McGenity et al., 2018). Isoprene can be considered as a secondary metabolite and may regulate the rigidity of the plasmatic membrane to protect the cell against external alterations (Loreto and Velikova, 2001; Ladygina et al., 2006). Also, noteworthy mentioning is the presence of heptadecane ( $\text{C}_{17}$ ) in PE01 (Tables S4 and S5), which corroborates the presence of cyanobacteria, likely responsible for the preponderance of microbial remains (Brocks and Summons, 2014; Ladygina et al., 2006).

Despite the significant presence of aromatics and lipids, CN samples exhibit an unusual abundance of lignin and aromatic compounds. This indicates that the organic fraction in these speleothems can have a range of sources, including microbial and fresh organic matter (plant-derived) from the overlying soil (Fig. 7). Concerning the lipid composition, the relatively high abundance of *n*-alkanoic and *n*-alkenoic acids did not allow identifying the source of the organic fraction in sample CN1, because they are predominant in fungi, plants, and animal tissues (Hilditch, 1956). However, the presence of 3,7,11-Trimethyl-dodeca-2,6,10-trienoic acid, a branched alkanoic acid (Table S4), does confirm the influence of bacterial biomass (Scherf and Rullkötter, 2009). The lipid fraction of CN2 is mainly composed of short-chain *n*-alkane/alkene pairs (Fig. 5, Table S5), pointing to cave microbiome as its source of organic matter (Blyth et al., 2008, 2011).

LB04 and MR02, albeit collected from different lava tubes (*Las Breñas* and *Montaña Rajada*, respectively), are dominated by steranes, peptides, and lipids, indicating the presence of microorganisms (Chen et al., 2020; Miller et al., 2022). In fact, the branched lipids identified in MR02 (Table S5), and the presence of heptadecane, are usually detected in cyanobacteria (Winters et al., 1969; Brocks and Summons, 2014), and in anaerobic phototrophic bacteria (Han and Calvin, 1969), being considered bacterial biomarkers (Kaneda, 1991). The presence of stigmasterane, sitosterol, and  $\alpha$ - $\beta$ -tocopherol (vitamin E) might indicate the contribution of organic matter from plants and micro-/macroalgae (Brendolise et al., 2011; Miller et al., 2020a; Volkman, 2003). The  $\alpha$ - $\beta$ -tocopherol is also produced by photosynthetic microorganisms like cyanobacteria (Niki and Abe, 2019), which is in fair agreement with the microbial community composition identified in MR02. It is worth remembering that this sampling site comprises a photosynthetic-based

biofilm collected in the twilight zone of *Montaña Rajada*. The presence of microbial biomarkers in both sampling sites (LB04 and MR02) may also be corroborated by the existence of short-chain *n*-alkane/alkene pairs (Table S5).

Our study indicates that the microorganisms associated with the secondary minerals of Lanzarote lava tubes are an important source of organic matter and primary biomarkers in speleothems (Fig. 7). Previous research conducted in various contexts has shown that microbial communities are known to be important contributors to biomarker records (Cardoso and Eglinton, 1983; Tremblay and Benner, 2006; Wakeham et al., 2003).

When exploring, for the first time, the relationships among organic families, microbial taxa, and cave minerals, significant ( $P < 0.05$ ) correlations were observed between the molecular data, mineralogical composition (independent variables), and the most abundant microbial phylotypes (dependent variables) at the order taxonomic level (Fig. 6). The first cluster obtained by PCA and defined by CN1 and CN2 from *Cueva de los Naturalistas* (Fig. 6A), shows a strong relation between the bacterial community and the presence of peptides, lignin, PAHs, and N-containing compounds, such as indole and pyridine (Fig. 6B). These products are commonly synthesized by plants (vegetation biomarkers), and their degradation through bacteria has been previously documented (Časaitė et al., 2020; Fetzner, 1998; Kaiser et al., 1996; Tomar et al., 2022). These N-compounds may act as signal molecule in biofilm development and preservation, virulence promotion, antibiotic resistance and cell formation (Melander et al., 2014). Some of the identified bacterial taxa, such as *Solirubrobacterales* and *Gemmatimonadales*, may contain a large number of biosynthetic gene clusters, which produce nonribosomal peptide synthetase, lassopeptides or bacteriocins (Waschulin et al., 2022). On the other hand, the presence of *Sphingobacteriales*, with specific PAH degradation mechanisms (Zhang et al., 2019), suggests that subsurface bacteria adapt their metabolism to use recalcitrant pyrogenic compounds, derived from the surface soil, as source of carbon and energy (Miller et al., 2020a, 2022).

The siliceous minerals from the basaltic rock (Andesine and Augite) and secondary fluorapatite, together with sterane compounds, whose precursor is the sterol, dominate the second cluster. Sterol is a well-known eukaryotic molecule synthesized by animals, plants and fungi (Weatherby and Carter, 2013). Only few bacterial species belonging to different phyla seem to produce sterols (*Bacteroidota*, *Cyanobacteriota*, *Planctomycetota*, *Pseudomonadota*, and *Verrucomicrobiota*), which are barely represented in cluster-II (Fig. 6B). Therefore, the presence of sterane in LB04 suggests the implication of cave microorganisms in the degradation of sterols derived from surface organisms reaching the cave via percolating water. It is known that sterols, like many polycyclic triterpenoids, are quite recalcitrant and their degradation products (i.e., steranes), are readily preserved in ancient sediments (Wei et al., 2016).

Aromatic compounds, such as benzoate identified in PE03, are almost exclusively associated with *Bacteroidales* in cluster-III (Fig. 6B). Sodium benzoate is a salt of benzoic acid, soluble in water and commonly used in the food industry due to its antifungal and antibacterial properties (Cao et al., 2009). This could explain the low microbial diversity observed in PE03 (Fig. 2), also consistent with the cultivation data, as no isolates were obtained for PE03. Zhuang et al. (2019) provide evidence for the involvement of *Bacteroidales* in aromatic compounds degradation, and proposed it as an attractive strategy for bioremediation of sites contaminated with aromatic compounds.

Halite and gypsum are linked to members of the phyla *Pseudomonadota* and *Cyanobacteriota*, the main bacteria identified in samples PE01 and MR02, collected in the twilight zone of the caves.

Furans and *n*-alkanoic acids (lipid family), abundantly identified in PE01 and PE03, are broadly present in lipids from a wide range of organisms, including some fish, plants, and microbes, protecting cell membranes from damaging agents (Lemke et al., 2020). This explains the correlation with lipid compounds and the microbial taxa observed in cluster-III, and suggests the adaptation of microorganisms to hostile

environments as lava tubes. Although with less significance, the correlation of polysaccharides in this cluster also supports this hypothesis, as glue-like compounds are essential molecules for biofilm formation, conferring protection, access to nutrients and adhesion to solid surfaces. They are an important survival strategy of microbial cells, allowing them to thrive in hostile niche conditions (Limoli et al., 2015).

Until now, studies have focused solely on exploring the correlation between physicochemical parameters and microbial diversity (Blyth et al., 2008; Dhami et al., 2018; Miller et al., 2016). However, the combined influence of mineral composition and organic compounds on subsurface microbial diversity has not been previously examined. This study, for the first time, demonstrates a clear relationship among the mineralogical composition, organic compounds, and microorganisms in the four lava tubes investigated in Lanzarote. The statistical approach employed in this work (PCA) reveals that subsurface microbiota is influenced by organic families and cave minerals. This finding opens up new avenues of research not just for understanding mineral biotic and abiotic alteration mechanisms, but also for using organic matter indicators (biomarkers) to predict microbial composition in terrestrial lava tubes.

Currently, >1300 potential entrances have been identified along lava flows in the Tharsis region of Mars (Wynne et al., 2022). The presented data is important in guiding potential research on extant microbial life in Martian lava tubes. It also aids, in the development of protocols, routines, and predictive models, offering valuable guidance on where and how to search for potential biosignatures on Mars. The microscopy techniques, DNA sequencing, and analytical biogeochemistry tools, particularly the analytical pyrolysis, used in this study can provide information to assess microbe-mineral interactions in Martian speleothems from molecular to macroscopic scales. However, it is crucial to emphasize the necessity of considering the conditions of the adjacent surface environment when interpreting the results, especially in the context of potential astrobiological implications for Mars.

#### CRediT authorship contribution statement

**Vera Palma:** Formal analysis, Writing – original draft. **José L. González-Pimentel:** Formal analysis, Writing – original draft. **Nicasio T. Jimenez-Morillo:** Data curation, Formal analysis, Methodology, Supervision, Writing – original draft, Writing – review & editing. **Francesco Sauro:** Data curation, Formal analysis, Methodology, Writing – original draft, Writing – review & editing. **Sara Gutiérrez-Patricio:** Formal analysis, Writing – original draft. **José M. De la Rosa:** Visualization, Writing – review & editing. **Ilaria Tomasi:** Formal analysis, Methodology, Writing – original draft, Writing – review & editing. **Matteo Massironi:** Data curation, Formal analysis, Methodology, Writing – original draft, Writing – review & editing. **Bogdan P. Onac:** Data curation, Formal analysis, Methodology, Writing – original draft, Writing – review & editing. **Igor Tiago:** Visualization, Writing – review & editing. **José A. González-Pérez:** Data curation, Writing – review & editing. **Leonila Laiz:** Validation, Writing – review & editing. **Ana T. Caldeira:** Supervision, Writing – review & editing. **Beatriz Cubero:** Visualization, Writing – review & editing. **Ana Z. Miller:** Conceptualization, Data curation, Formal analysis, Funding acquisition, Methodology, Project administration, Resources, Supervision, Writing – original draft, Writing – review & editing.

#### Declaration of competing interest

The authors declare no competing financial interest or personal relationships that could have influenced the work reported in this paper.

#### Data availability

The raw data generated for this study are available at the NCBI Sequence Read Archive (SRA) database under accession number

PRJNA816077, and GenBank database under accession numbers OQ804791 - OQ804805 and OQ805860 - OQ805866. Supplementary materials contain a detailed description of the geology of Lanzarote, the sampled lava tubes, as well as additional figures and tables.

#### Acknowledgments

This work received support from the Spanish Ministry of Science and Innovation (MCIN) under the research project TUBOLAN PID2019-108672RJ-I00 funded by MCIN/AEI/10.13039/501100011033. The financial support from the Portuguese Foundation for Science and Technology (FCT) under the MICROCENO project (DOI 10.54499/PTD C/CTA-AMB/0608/2020) and the HERCULES Laboratory of the University of Évora (DOI 10.54499/UIIDP/04449/2020) are also acknowledged. S.G-P was supported by the Spanish National Research Council (CSIC) through the intramural project PIE\_20214AT021. N.T.J.M. and A. Z.M. were supported by Ramón y Cajal contracts (RyC2021-031253-I and RYC2019-026885-I, respectively) from the MCIN. The authors would like to thank the Lanzarote Geopark, the Timanfaya National Park and the Cabildo of Lanzarote for the sampling permits and logistic assistance on site. The authors are also grateful to Gustavo Santana Gomez, president of the Vulcan Vertical Club for his speleological guidance during the sampling campaigns. The technical assistance of Juana Muñoz is also acknowledged.

#### Appendix A. Supplementary data

Supplementary data to this article can be found online at <https://doi.org/10.1016/j.scitotenv.2023.169583>.

#### References

- Almendros, G., Hernández, Z., Sanz, J., Rodríguez-Sánchez, S., Jiménez-González, M.A., González-Pérez, J.A., 2018. Graphical statistical approach to soil organic matter resilience using analytical pyrolysis data. *J. Chromatogr. A* 1533, 164–173.
- Ansari, A.H., 2023. Detection of organic matter on Mars, results from various Mars missions, challenges, and future strategy: a review. *Front. Astron. Space Sci.* 10, 1075052.
- Baqué, M., Backhaus, T., Meessen, J., Hanke, F., Böttger, U., et al., 2022. Biosignature stability in space enables their use for life detection on Mars. *Sci. Adv.* 8, eabn7412.
- Biderre-Petit, C., Hochart, C., Gardon, H., Dugat-Bony, E., Terrat, S., Jouan-Dufournel, I., et al., 2020. Analysis of bacterial and archaeal communities associated with Fogo volcanic soils of different ages. *FEMS Microbiol. Ecol.* 96.
- Biswas, J., Mandal, S., Paul, A.K., 2015. Production, partial purification and some biophysicochemical properties of EPS produced by *Halomonas xianhensis* SUR308 isolated from a saltern environment. *J. Biol. Act. Prod. Nat.* 5, 108–119.
- Blair, D.M., Chappaz, L., Sood, R., Milbury, C., Bobet, A., Melosh, H.J., et al., 2017. The structural stability of lunar lava tubes. *Icarus* 282, 47–55.
- Blyth, A.J., Frisia, S., 2008. Molecular evidence for bacterial mediation of calcite formation in cold high-altitude caves. *Geomicrobiol. J.* 25, 101–111.
- Blyth, A.J., Baker, A., Collins, M.J., Penkman, K.E., Gilmour, M.A., Moss, J.S., et al., 2008. Molecular organic matter in speleothems and its potential as an environmental proxy. *Quat. Sci. Rev.* 27, 905–921.
- Blyth, A.J., Baker, A., Thomas, L.E., Van Calsteren, P., 2011. A 2000-year lipid biomarker record preserved in a stalagmite from north-west Scotland. *J. Quat. Sci.* 26, 326–334.
- Boschker, H.T.S., Middelburg, J.J., 2002. Stable isotopes and biomarkers in microbial ecology. *FEMS Microbiol. Ecol.* 40, 85–95.
- Brendolise, C., Yauk, Y.-K., Eberhard, E.D., Wang, M., Chagne, D., Andre, C., et al., 2011. An unusual plant triterpene synthase with predominant  $\alpha$ -amyrin-producing activity identified by characterizing oxidosqualene cyclases from *Malus domestica*. *FEBS J.* 278, 2485–2499.
- Brocks, J.J., Summons, R.E., 2014. Sedimentary hydrocarbons, biomarkers for early life. In: Holland, H.D., Turekian, K.K. (Eds.), *Treatise on Geochemistry* (Second Edition). Elsevier, Oxford, pp. 61–103.
- Bolyen, E., Rideout, J.R., Dillon, M.R., Bokulich, N.A., Abnet, C.C., Al-Ghalthi, G.A., et al., 2019. Reproducible, interactive, scalable and extensible microbiome data science using QIIME 2. *Nat. Biotechnol.* 37, 852–857. <https://doi.org/10.1038/s41587-019-0209-9>.
- Callahan, B.J., McMurdie, P.J., Rosen, M.J., Han, A.W., Johnson, A.J., Holmes, S.P., 2016. DADA2: high-resolution sample inference from Illumina amplicon data. *Nat. Methods* 13, 581–583.
- Cao, B., Nagarajan, K., Loh, K.-C., 2009. Biodegradation of aromatic compounds: current status and opportunities for biomolecular approaches. *Appl. Microbiol. Biotechnol.* 85, 207–228.
- Cardoso, J.N., Eglinton, G., 1983. The use of hydroxyacids as geochemical indicators. *Geochim. Cosmochim. Acta* 47, 723–730.



- Carr, M.H., Head, J.W., 2010. Geologic history of Mars. *Earth Planet. Sci. Lett.* 294, 185–203.
- Časaitė, V., Stanislauskienė, R., Vaitekūnas, J., Tauraitė, D., Rutkienė, R., Gasparavičiūtė, R., et al., 2020. Microbial degradation of pyridine: a complete pathway in *Arthrobacter* sp. strain 68b deciphered. *Appl. Environ. Microbiol.* 86, e00902-20.
- Chan, M.A., Hinman, N.W., Potter-McIntyre, S.L., Schubert, K.E., Gillams, R.J., Awramik, S.M., et al., 2019. Deciphering biosignatures in planetary contexts. *Astrobiology* 19, 1075–1102.
- Chen, Y.-H., Chang, Y.-C., Chen, Y.-H., Zheng, L.-G., Huang, P.-C., Huynh, T.-H., et al., 2020. Natural products from octocorals of the genus *Dendronephthya* (family Nephtheidae). *Molecules* 25, 5957.
- Cuezva, S., Fernandez-Cortes, A., Porca, E., Pašić, L., Jurado, V., Hernández Mariné, M., et al., 2012. The biogeochemical role of Actinobacteria in Altamira Cave, Spain. *FEMS Microbiol. Ecol.* 81, 281–290.
- De la Rosa, J.M., Jiménez-Morillo, N.T., González-Pérez, J.A., Almendros, G., Vieira, D., Knicker, H.E., et al., 2019. Mulching-induced preservation of soil organic matter quality in a burnt eucalypt plantation in central Portugal. *J. Environ. Manag.* 231, 1135–1144.
- Dhami, N.K., Mukherjee, A., ELJ, Watkin, 2018. Microbial diversity and mineralogical-mechanical properties of calcitic cave speleothems in natural and in vitro biomineralization conditions. *Front. Microbiol.* 9, 40.
- Donahue, J.M., Williams, N.M., Sells, S.F., Labeda, D.P., 2002. *Crossiella equi* sp. nov., isolated from equine placentas. *Int. J. Syst. Evol. Microbiol.* 52, 2169–2173.
- Douglas, G.M., Maffei, V.J., Zaneveld, J.R., Yurgel, S.N., Brown, J.R., Taylor, C.M., et al., 2020. PICRUST2 for prediction of metagenome functions. *Nat. Biotechnol.* 38, 685–688. <https://doi.org/10.1038/s41587-020-0548-6>.
- Echigo, A., Hino, M., Fukushima, T., Mizuki, T., Kamakura, M., Usami, R., 2005. Endospores of halophilic bacteria of the family *Bacillaceae* isolated from non-saline Japanese soil may be transported by Kosa event (Asian dust storm). *Saline Syst.* 1, 8.
- Fetzner, S., 1998. Bacterial degradation of pyridine, indole, quinoline, and their derivatives under different redox conditions. *Appl. Microbiol. Biotechnol.* 49, 237–250.
- Fiebig, K., Friedrich, B., 1989. Purification of the F420-reducing hydrogenase from *Methanosarcina barkeri* (strain Fusaro). *Eur. J. Biochem./FEBS* 184, 79–88.
- Fishman, B., Bevilacqua, J.G., Hahn, A.S., Morgan-Lang, C., Wagner, N., Gadson, O., McAdam, A.C., Bleacher, J., Achilles, C., Knudson, C., Millan, M.M., 2023. Extreme niche partitioning and microbial dark matter in a Mauna Loa lava tube. *J. Geophys. Res. Planets* 128, e2022JE007283.
- Forti, P., 2005. Genetic processes of cave minerals in volcanic environments: an overview. *J. Cave Karst Stud.* 67, 3–13.
- Fry, B., 2006. *Stable Isotope Ecology*. Springer, New York.
- García, G.M., Márquez, G.M.A., Moreno, H.C.X., 2016. Characterization of bacterial diversity associated with calcareous deposits and drip-waters, and isolation of calcifying bacteria from two Colombian mines. *Microbiol. Res.* 182, 21–30.
- Gonzalez-Pimentel, J.L., Martín-Pozas, T., Jurado, V., Miller, A., Caldeira, A., Fernandez-Lorenzo, O., et al., 2021. Prokaryotic communities from a lava tube cave in La Palma Island (Spain) are involved in the biogeochemical cycle of major elements. *PeerJ* 9, e11386.
- Gonzalez-Pimentel, J.L., Miller, A.Z., Jurado, V., Laiz, L., Pereira, M.F., Saiz-Jimenez, C., 2018. Yellow coloured mats from lava tubes of La Palma (Canary Islands, Spain) are dominated by metabolically active Actinobacteria. *Sci. Rep.* 8, 1–11.
- Greeley, R., 1971. Lava tubes and channels in the lunar Marius Hills. *The Moon* 3, 289–314.
- Großkopf, R., Janssen, P.H., Liesack, W., 1998. Diversity and structure of the methanogenic community in anoxic rice paddy soil microcosms as examined by cultivation and direct 16S rRNA gene sequence retrieval. *Appl. Environ. Microbiol.* 64, 960–969.
- Han, J., Calvin, M., 1969. Hydrocarbon distribution of algae and bacteria, and microbiological activity in sediments. *Proc. Natl Acad. Sci. USA* 64, 436–443.
- Han, Y., Sun, B., Yan, H., Tucker, M.E., Zhao, Y., Zhou, J., et al., 2020. Biomineralization of carbonate minerals induced by the moderate halophile *Staphylococcus warneri* YXY2. *Crystals* 10, 58.
- Haruyama, J., Hioki, K., Shirao, M., Morota, T., Hiesinger, H., van der Bogert, C., et al., 2009. Possible lunar lava tube skylight observed by SELENE cameras. *Geophys. Res. Lett.* 36.
- Hashimoto, M., Hossain, S., 2018. Fatty acids: from membrane ingredients to signaling molecules. In: Viduranga, W. (Ed.), *Biochemistry and Health Benefits of Fatty Acids*. IntechOpen, Rijeka (pp. Ch. 2).
- Hata, T., Saracho, A.C., Haigh, S.K., Yoneda, J., Yamamoto, K., 2020. Microbial-induced carbonate precipitation applicability with the methane hydrate-bearing layer microbe. *J. Nat. Gas Sci. Eng.* 81, 103490.
- Hauschild, A.H.W., Holdeman, L.V., 1974. *Clostridium celatum* sp. nov., isolated from normal human feces. *Int. J. Syst. Evol. Microbiol.* 24, 478–481.
- Hayes, J.M., 2018. Fractionation of carbon and hydrogen isotopes in biosynthetic processes. In: John, W.V., David, R.C. (Eds.), *Stable Isotope Geochemistry*. De Gruyter, Berlin, Boston, pp. 225–278.
- Hilditch, T.P., 1956. *The Chemical Constitution of Natural Fats*. Chapman & Hall, New York, USA.
- Huerta, P., Martín-Pérez, A., Martín-García, R., Rodríguez-Berriquete, Á., La Iglesia, Fernández Á., Alonso-Zarza, A.M., 2019. Gypsum speleothems in lava tubes from Lanzarote (Canary Islands). Ion sources and pathways. *Sediment. Geol.* 383, 136–147.
- Huidobro, J., Aramendia, J., Arana, G., Madariaga, J.M., 2022. Reviewing in situ analytical techniques used to research Martian geochemistry: from the Viking Project to the MMX future mission. *Anal. Chim. Acta* 1197, 339499.
- Idris, I., Rustandi, B., Sulistiyani, T.R., Rahmat, A., Sudiana, I.M., 2022. Bioprospecting Ureolytic Rock Bacteria for Calcium Carbonate Precipitation Inducer.
- Jain, S., Caforio, A., Driessen, A.J.M., 2014. Biosynthesis of archaeal membrane ether lipids. *Front. Microbiol.* 5.
- Jian, S.L., Xu, L., Meng, F.X., Sun, C., Xu, X.W., 2021. *Euzebya pacifica* sp. nov., a novel member of the class Nitriliruptoria. *Int. J. Syst. Evol. Microbiol.* 71.
- Jiménez-Morillo, N.T., Spangenberg, J.E., Miller, A.Z., Jordán, A., Zavala, L.M., González-Vila, F.J., et al., 2017. Wildfire effects on lipid composition and hydrophobicity of bulk soil and soil size fractions under *Quercus suber* cover (SW-Spain). *Environ. Res.* 159, 394–405.
- Jiménez-Morillo, N.T., González-Pérez, J.A., Almendros, G., De la Rosa, J.M., Waggoner, D.C., Jordán, A., et al., 2018. Ultra-high resolution mass spectrometry of physical speciation patterns of organic matter in fire-affected soils. *J. Environ. Manag.* 225, 139–147.
- Jiménez-Morillo, N.T., Almendros, G., De la Rosa, J.M., Jordán, A., Zavala, L.M., Granged, A.J.P., et al., 2020. Effect of a wildfire and of post-fire restoration actions in the organic matter structure in soil fractions. *Sci. Total Environ.* 728, 138715.
- Juretschko, S., Timmermann, G., Schmid, M., Schleifer, K.H., Pommerening-Röser, A., Koops, H.P., et al., 1998. Combined molecular and conventional analyses of nitrifying bacterium diversity in activated sludge: *Nitrosococcus mobilis* and *Nitrospira*-like bacteria as dominant populations. *Appl. Environ. Microbiol.* 64, 3042–3051.
- Kaiser, J.P., Feng, Y., Bollag, J.M., 1996. Microbial metabolism of pyridine, quinoline, acridine, and their derivatives under aerobic and anaerobic conditions. *Microbiol. Rev.* 60, 483–498.
- Kaneda, T., 1991. Iso- and anteiso-fatty acids in bacteria: biosynthesis, function, and taxonomic significance. *Microbiol. Rev.* 55, 288–302.
- Kelly, L.C., Cockell, C.S., Thorsteinsson, T., Marteinsson, V., Stevenson, J., 2014. Pioneer microbial communities of the Fimmvörðuháls lava flow, Eyjafjallajökull, Iceland. *Microbiol. Ecol.* 68, 504–518.
- Kim, O.S., Cho, Y.J., Lee, K., Yoon, S.H., Kim, M., Na, H., et al., 2012. Introducing EzTaxon-e: a prokaryotic 16S rRNA gene sequence database with phylogenies that represent uncultured species. *Int. J. Syst. Evol. Microbiol.* 62, 716–721.
- Koning, K., McFarlane, R., Gosse, J.T., Lawrence, S., Carr, L., Horne, D., et al., 2022. Biomineralization in cave bacteria—popcorn and soda straw crystal formations, morphologies, and potential metabolic pathways. *Front. Microbiol.* 13.
- Kosznik-Kwasnicka, K., Golec, P., Jaroszewicz, W., Lubomska, D., Piechowicz, L., 2022. Into the unknown: microbial communities in caves, their role, and potential use. *Microorganisms* 10.
- Kurahashi, M., Fukunaga, Y., Sakiyama, Y., Harayama, S., Yokota, A., 2010. *Euzebya tangerina* gen. nov., sp. nov., a deeply branching marine actinobacterium isolated from the sea cucumber *Holothuria edulis*, and proposal of *Euzebyaceae* fam. nov., *Euzebyales* ord. nov. and *Nitriliruptoridae* subclassis nov. *Int. J. Syst. Evol. Microbiol.* 60, 2314–2319.
- Labeda, D.P., 2001. *Crossiella* gen. Nov., a new genus related to *Streptoalloteichus*. *Int. J. Syst. Evol. Microbiol.* 51, 1575–1579.
- Ladygina, N., Dedyukhina, E.G., Vainshtein, M.B., 2006. A review on microbial synthesis of hydrocarbons. *Process Biochem.* 41, 1001–1014.
- Lafuente, B., Downs, R.T., Yang, H., Stone, N., 2015. 1. The power of databases: the RRUFF project. Highlights in mineralogical crystallography. *De Gruyter (O)* 1–30.
- Langille, M.G.I., Zaneveld, J., Caporaso, J.G., McDonald, D., Knights, D., Reyes, J.A., et al., 2013. Predictive functional profiling of microbial communities using 16S rRNA marker gene sequences. *Nat. Biotechnol.* 31, 814–821.
- Lavoie, K.H., Winter, A.S., Read, K.J., Hughes, E.M., Spilde, M.N., Northup, D.E., 2017. Comparison of bacterial communities from lava cave microbial mats to overlying surface soils from Lava Beds National Monument, USA. *PLoS One* 12, e0169339.
- Lemke, R.A.S., Olson, S.M., Morse, K., Karlen, S.D., Higbee, A., Beebe, E.T., et al., 2020. A bacterial biosynthetic pathway for methylated furan fatty acids. *J. Biol. Chem.* 295, 9786–9801.
- Leslie, K., van Geffen, P.W.G., MacFarlane, B., Oates, C.J., Kyser, T.K., Fowle, D.A., 2013. Biogeochemical indicators of buried mineralization under cover, Talbot VMS Cu–Zn prospect, Manitoba. *Appl. Geochem.* 37, 190–202.
- Léveillé, R.J., Datta, S., 2010. Lava tubes and basaltic caves as astrobiological targets on Earth and Mars: a review. *Planet. Space Sci.* 58, 592–598.
- Li, Q., Zhang, B., Yang, X., Ge, Q., 2018. Deterioration-associated microbiome of stone monuments: structure, variation, and assembly. *Appl. Environ. Microbiol.* 84.
- Limoli, D.H., Jones, C.J., Wozniak, D.J., 2015. Bacterial extracellular polysaccharides in biofilm formation and function. *Microbiol. Spectr.* 3.
- Loreto, F., Velikova, V., 2001. Isoprene produced by leaves protects the photosynthetic apparatus against ozone damage, quenches ozone products, and reduces lipid peroxidation of cellular membranes. *Plant Physiol.* 127, 1781–1787.
- Lozupone, C., Knight, R., 2005. UniFrac: a new phylogenetic method for comparing microbial communities. *Appl. Environ. Microbiol.* 71, 8228–8235.
- Lozupone, C.A., Hamady, M., Kelley, S.T., Knight, R., 2007. Quantitative and qualitative beta diversity measures lead to different insights into factors that structure microbial communities. *Appl. Environ. Microbiol.* 73, 1576–1585.
- Ma, L., Huang, X., Wang, H., Yun, Y., Cheng, X., Liu, D., et al., 2021. Microbial interactions drive distinct taxonomic and potential metabolic responses to habitats in karst cave ecosystem. *Microbiol. Spectr.* 9, e0115221.
- Martín, J., Díaz, M., 1984. El tubo vulcanico de Los Naturalistas. *Lapiaz* 13, 51–54.
- Martínez-Frías, J., 2014. Search for life on Mars: an astrogeological approach. In: Kolb, V. (Ed.), *Astrobiology: An Evolutionary Approach*. CRC Press, p. 504.
- Martínez-Frías, J., Amaral, G., Vázquez, L., 2006. Astrobiological significance of minerals on Mars surface environment. *Rev. Environ. Sci. Biotechnol.* 5, 219–231.
- Martínez-Frías, J., Mederos, E.M., Lunar, R., 2017. The scientific and educational significance of geoparks as planetary analogues: the example of Lanzarote and

- Chinijo Islands UNESCO Global Geopark. International Union of Geological Sciences 40, 343–347.
- Martin-Pozas, T., Gonzalez-Pimentel, J.L., Jurado, V., Laiz, L., Cañaveras, J.C., Fernandez-Cortes, A., Cuezva, S., Sanchez-Moral, S., Saiz-Jimenez, C., 2023. *Crossiella*, a rare *Actinomyces* genus, abundant in the environment. *Appl. Biosci.* 2, 194–210.
- Mateo-Mederos, E., Martínez-Frías, J., Vegas, J., 2019. Lanzarote and Chinijo Islands Geopark: From Earth to Space. Springer.
- McGenity, T.J., Crombie, A.T., Murrell, J.C., 2018. Microbial cycling of isoprene, the most abundantly produced biological volatile organic compound on Earth. *ISME J.* 12, 931–941.
- Melander, R.J., Minvielle, M.J., Melander, C., 2014. Controlling bacterial behavior with indole-containing natural products and derivatives. *Tetrahedron* 70, 6363–6372.
- Meyzen, C., Massironi, M., Pozzobon, R., Dal, Zilio L., 2015. Are terrestrial plumes from motionless plates analogous to Martian plumes feeding the giant shield volcanoes? In: Platz, T., Massironi, M., Byrne, P.K., Hiesinger, H. (Eds.), *Volcanism and Tectonism Across the Inner Solar System*. 401. London, Special Publications, Geological Society, pp. 107–126.
- Miller, A.Z., De la Rosa, J.M., Jiménez-Morillo, N.T., Pereira, M.F.C., González-Pérez, J. A., Calaforra, J.M., et al., 2016. Analytical pyrolysis and stable isotope analyses reveal past environmental changes in coralloid speleothems from Easter Island (Chile). *J. Chromatogr. A* 1461, 144–152.
- Miller, A.Z., Gonzalez-Pimentel, J.L., Stahl, S., Castro-Wallace, S., Sauro, F., Pozzobon, R., et al., 2018. Exploring possible Mars-like microbial life in a lava tube from Lanzarote: preliminary results of in-situ DNA-based analysis as part of the PANGAEA-X test campaign. EGU General Assembly Conference Abstracts 1258.
- Miller, A.Z., De la Rosa, J.M., Jiménez-Morillo, N.T., Pereira, M.F.C., Gonzalez-Perez, J. A., Knicker, H., et al., 2020a. Impact of wildfires on subsurface volcanic environments: new insights into speleothem chemistry. *Sci. Total Environ.* 698, 134321.
- Miller, A.Z., García-Sánchez, A.M., L. Coutinho, M., Costa Pereira, M.F., Gázquez, F., Calaforra, J.M., et al., 2020b. Colored microbial coatings in show caves from the Galapagos Islands (Ecuador): first microbiological approach. *Coatings* 10, 1134.
- Miller, A.Z., Jiménez-Morillo, N.T., Coutinho, M.L., Gázquez, F., Palma, V., Sauro, F., et al., 2022. Organic geochemistry and mineralogy suggest anthropogenic impact in speleothem chemistry from volcanic show caves of the Galapagos. *iScience* 25, 104556.
- Montoriol-Pous, J., De Mier, J., Montserrat i Nebot, A., 1991. Estudi vulcano-espeleològic de la Cueva de las Palomas (Lanzarote, Canàries). *Espeleòleg* 39, 11–18.
- Nicolosi, G., Gonzalez-Pimentel, J.L., Piano, E., Isaia, M., Miller, A.Z., 2023. First insights into the bacterial diversity of Mount Etna volcanic caves. *Microb. Ecol.* 86, 1632–1645.
- Niki, E., Abe, K., 2019. Vitamin E: Structure, Properties and Functions. *Chemistry and Nutritional Benefits*. Royal Society of Chemistry, Vitamin E, pp. 1–11.
- Northup, D., Melim, L., Spilde, M., Hathaway, J., Garcia, M., Moya, M., et al., 2011. Lava cave microbial communities within mats and secondary mineral deposits: implications for life detection on other planets. *Astrobiology* 11, 601–618.
- Onac, B.P., Forti, P., 2011. Minerogenetic mechanisms occurring in the cave environment: an overview. *Int. J. Speleol.* 40 (2), 79–98.
- Pielou, E.C., 1966. The measurement of diversity in different types of biological collections. *J. Theor. Biol.* 13, 131–144.
- Prakash, E.A., Hromádková, T., Jabir, T., Vipindas, P., Krishnan, K., Hatha, A.M., et al., 2022. Dissemination of multidrug resistant bacteria to the polar environment-role of the longest migratory bird Arctic tern (*Sterna paradisaea*). *Sci. Total Environ.* 815, 152727.
- Quast, C., Pruesse, E., Yilmaz, P., Gerken, J., Schweer, T., Yarza, P., et al., 2013. The SILVA ribosomal RNA gene database project: improved data processing and web-based tools. *Nucleic Acids Res.* 41, D590–D596.
- Rainey, F., Hollen, B.J., Small, A., Genus, I., 2009. *Clostridium Prazmowski 1880*, 23<sup>AL</sup>. In: Vos, P.D., Garrity, G.M., Jones, D., Krieg, N.R., Ludwig, W., Rainey, F.A., et al. (Eds.), *Bergey's Manual of Systematic Bacteriology*, Vol. 3. The Firmicutes. Springer, pp. 738–828.
- Reinhart, M., Goetz, W., Thiel, V., 2020. Testing flight-like pyrolysis gas chromatography/mass spectrometry as performed by the Mars Organic Molecule Analyzer onboard the ExoMars 2020 rover on Oxia Planum analog samples. *Astrobiology* 20, 415–428.
- Rice, M.S., Bell III, J.F., Cloutis, E.A., Wang, A., Ruff, S.W., Craig, M.A., Bailey, D.T., Johnson, J.R., de Souza Jr. PA, Farrand WH., 2010. Silica-rich deposits and hydrated minerals at Gusev Crater, Mars: Vis-NIR spectral characterization and regional mapping. *Icarus* 205 (2), 375–395.
- Riquelme, C., Marshall Hathaway, J.J., Enes Dapkevicius, MdL, Miller, A.Z., Kooser, A., Northup, D.E., et al., 2015. Actinobacterial diversity in volcanic caves and associated geomicrobiological interactions. *Front. Microbiol.* 6, 1342.
- Rosselló-Mora, R., Amann, R., 2001. The species concept for prokaryotes. *FEMS Microbiol. Rev.* 25, 39–67.
- Sauro, F., Cappelletti, M., Ghezzi, D., Columbu, A., Hong, P.Y., Zowawi, H.M., et al., 2018. Microbial diversity and biosignatures of amorphous silica deposits in orthoquartzite caves. *Sci. Rep.* 8.
- Sauro, F., Pozzobon, R., Santagata, T., Tomasi, I., Tonello, M., Martínez-Frías, J., et al., 2019. Volcanic Caves of Lanzarote: A Natural Laboratory for Understanding Volcano-Speleogenetic Processes and Planetary Caves. *From Earth to Space*. Springer, Lanzarote and Chinijo Islands Geopark, pp. 125–142.
- Sauro, F., Pozzobon, R., Massironi, M., De Berardinis, P., Santagata, T., De Waele, J., 2020. Lava tubes on Earth, Moon and Mars: a review on their size and morphology revealed by comparative planetology. *Earth Sci. Rev.* 209, 103288.
- Sauro, F., Payler, S.J., Massironi, M., Pozzobon, R., Hiesinger, H., Mangold, N., et al., 2023. Training astronauts for scientific exploration on planetary surfaces: the ESA PANGAEA programme. *Acta Astronaut.* 204, 222–238.
- Scherf, A.-K., Rullkötter, J., 2009. Biogeochemistry of high salinity microbial mats – part 1: lipid composition of microbial mats across intertidal flats of Abu Dhabi, United Arab Emirates. *Org. Geochem.* 40, 1018–1028.
- Selensky, M.J., Masterson, A.L., Blank, J.G., Lee, S.C., Osburn, M.R., 2021. Stable carbon isotope depletions in lipid biomarkers suggest subsurface carbon fixation in lava caves. *J. Geophys. Res. Biogeosci.* 126, e2021JG006430.
- Shannon, C.E., 1948. A mathematical theory of communication. *Bell Syst. Tech. J.* 27, 379–423.
- Squyres, S.W., Arvidson, R.E., Ruff, S., Gellert, R., Morris, R.V., Ming, D.W., Crumpler, L., Farmer, J., Des Marais, D.J., Yen, A., McLennan, S., 2008. Discovery of silica-rich deposits on Mars by the Spirit Rover. *Science* 320, 1063–1067.
- Stackebrandt, E., 2003. The richness of prokaryotic diversity: there must be a species somewhere. *Food Technol. Biotechnol.* 41, 17–22.
- Teehera, K.B., Jungbluth, S.P., Onac, B.P., Acosta-Maeda, T.E., Hellebrand, E., Misra, A. K., Pflitsch, A., Rappé, M.S., Smith, S.M., Telus, M., Schorghofer, N., 2018. Cryogenic minerals in Hawaiian lava tubes: a geochemical and microbiological exploration. *Geomicrobiol. J.* 35 (3), 227–241.
- Thijs, S., Op De Beeck, M., Beckers, B., Truyens, S., Stevens, V., Van Hamme, J.D., Weyens, M., Vangronsveld, J., 2017. Comparative evaluation of four bacteria-specific primer pairs for 16S rRNA gene surveys. *Front. Microbiol.* 8, 494.
- Tomar, S.K., Kumar, R., Chakraborty, S., 2022. Simultaneous biodegradation of pyridine, indole, and ammonium along with phenol and thiocyanate by aerobic granular sludge. *J. Hazard. Mater.* 422, 126861.
- Tremblay, L., Benner, R., 2006. Microbial contributions to N-immobilization and organic matter preservation in decaying plant detritus. *Geochim. Cosmochim. Acta* 70, 133–146.
- Velikonja, B., Tkavc, R., Pašić, L., 2014. Diversity of cultivable bacteria involved in the formation of macroscopic microbial colonies (Cave silver) on the walls of a cave in Slovenia. *Int. J. Speleol.* 43, 45–56.
- Volkman, J., 2003. Sterols in microorganisms. *Appl. Microbiol. Biotechnol.* 60, 495–506.
- Wakeham, S.G., Lewis, C.M., Hopmans, E.C., Schouten, S., Sinninghe Damsté, J.S., 2003. Archaea mediate anaerobic oxidation of methane in deep euxinic waters of the Black Sea. *Geochim. Cosmochim. Acta* 67, 1359–1374.
- Waschulin, V., Borsetto, C., James, R., Newsham, K.K., Donadio, S., Corre, C., et al., 2022. Biosynthetic potential of uncultured Antarctic soil bacteria revealed through long-read metagenomic sequencing. *ISME J.* 16, 101–111.
- Wasimuddin, Schlaeppli, K., Ronchi, F., Leib, S.L., Erb, M., Ramette, A., 2020. Evaluation of primer pairs for microbiome profiling from soils to humans within the One Health framework. *Mol. Ecol. Resour.* 20, 1558–1571.
- Weatherby, K., Carter, D., 2013. Chromera velia: the missing link in the evolution of parasitism. *Adv. Appl. Microbiol.* 85, 119–144.
- Wei, J.H., Yin, X., Welandar, P.V., 2016. Sterol synthesis in diverse bacteria. *Front. Microbiol.* 7, 990.
- Westall, F., Cavalazzi, B., 2011. Biosignatures in rocks. In: Reitner, Joachim, Thiel, Volker (Eds.), *Encyclopedia of Geobiology*, 1st edition XXVIII. Springer-Verlag, p. 482. (928).
- Westall, F., de Ronde, C.E., Southam, G., Grassineau, N., Colas, M., Cockell, C., et al., 2006. Implications of a 3.472–3.333 Gyr-old subaerial microbial mat from the Barberton greenstone belt, South Africa for the UV environmental conditions on the early Earth. *Philos. Trans. R. Soc. Lond. Ser. B Biol. Sci.* 361, 1857–1875.
- Westall, F., Foucher, F., Bost, N., Bertrand, M., Loizeau, D., Vago, J.L., et al., 2015. Biosignatures on Mars: what, where, and how? Implications for the search for Martian life. *Astrobiology* 15, 998–1029.
- White, T.J., Bruns, T., Lee, S., Taylor, J., 1990. Amplification and direct sequencing of fungal ribosomal RNA genes for phylogenetics. In: Innis, M.A., Gelfand, D.H., Sninsky, J.J., White, T.J. (Eds.), *PCR Protocols: A Guide to Methods and Applications*. Academic Press, London, pp. 315–322.
- Whitcar, M.J., 1999. Carbon and hydrogen isotope systematics of bacterial formation and oxidation of methane. *Chem. Geol.* 161, 291–314.
- Winters, K., Parker, P.L., Van Baalen, C., 1969. Hydrocarbons of blue-green algae: geochemical significance. *Science* 163, 467–468.
- Wynne, J.J., Mylroie, J.E., Titus, T.N., Malaska, M.J., Buczkowski, D.L., Buhler, P.B., et al., 2022. Planetary caves: a solar system view of processes and products. *J. Geophys. Res. Planets* 127, e2022JE007303.
- Xia, J., Ling, S.-K., Wang, X.-Q., Chen, G.-J., Du, Z.-J., 2016. *Aliifodinibius halophilus* sp. nov., a moderately halophilic member of the genus *Aliifodinibius*, and proposal of *Balneolaceae* fam. nov. *Int. J. Syst. Evol. Microbiol.* 66, 2225–2233.
- Yin, Q., Zhang, L., Song, Z.M., Wu, Y., Hu, Z.L., Zhang, X.H., et al., 2018. *Euzebya rosea* sp. nov., a rare actinobacterium isolated from the East China Sea and analysis of two genome sequences in the genus *Euzebya*. *Int. J. Syst. Evol. Microbiol.* 68, 2900–2905.
- Yoon, S.H., Ha, S.M., Kwon, S., Lim, J., Kim, Y., Seo, H., et al., 2017. Introducing EzBioCloud: a taxonomically united database of 16S rRNA gene sequences and whole-genome assemblies. *Int. J. Syst. Evol. Microbiol.* 67, 1613–1617.
- Zhang, S., Hu, Z., Wang, H., 2019. Metagenomic analysis exhibited the co-metabolism of polycyclic aromatic hydrocarbons by bacterial community from estuarine sediment. *Environ. Int.* 129, 308–319.
- Zhuang, L., Tang, Z., Ma, J., Yu, Z., Wang, Y., Tang, J., 2019. Enhanced anaerobic biodegradation of benzoate under sulfate-reducing conditions with conductive iron-oxides in sediment of Pearl River Estuary. *Front. Microbiol.* 10.